Atmos. Chem. Phys., 24, 13151–13182, 2024
https://doi.org/10.5194/acp-24-13151-2024


Atmospheric Chemistry and Physics
Open Access
EGU



# Measurement report: Long-term measurements of surface ozone and trends in semi-natural sub-Saharan African ecosystems

**Hagninou Elagnon Venance Donnou[1], Aristide Barthélémy Akpo[1], Money Ossohou[2,3], Claire Delon[4], Véronique Yoboué[3], Dungall Laouali[5], Marie Ouafo-Leumbe[6], Pieter Gideon Van Zyl[7], Ousmane Ndiaye[8], Eric Gardrat[4], Maria Dias-Alves[4], and Corinne Galy-Lacaux[4]**

[1]Laboratoire de Physique du Rayonnement, Faculté des Sciences et Techniques, Université d'Abomey-Calavi, Cotonou, 01 B.P. 526, Benin
[2]Department of Physics, University of Man, Man, Côte d'Ivoire
[3]Laboratoire des Sciences de la Matière, de l'Environnement et de l'Energie Solaire, Université Félix Houphouët-Boigny, Abidjan, Côte d'Ivoire
[4]Laboratoire d'Aérologie, Université Toulouse III – Paul Sabatier, CNRS, Toulouse, 31400, France
[5]Laboratoire de Climat-Environnement et Matériaux-Rayonnement, Faculté des Sciences et Techniques, Université Abdou Moumouni, Niamey, BP 10662, Niger
[6]Department of Earth Sciences, Faculty of Sciences, University of Douala, Douala, P.O. Box 2701, Cameroon
[7]Atmospheric Chemistry Research Group, Chemical Resource Beneficiation, North-West University, Potchefstroom, 2520, South Africa
[8]Centre de Recherches Zootechniques de Dahra, Institut Sénégalais de Recherches Agricoles, Dahra, Senegal

**Correspondence:** Hagninou Elagnon Venance Donnou (donhelv@yahoo.fr) and Corinne Galy-Lacaux (corinne.galy-lacaux@aero.obs-mip.fr)

Received: 31 January 2024 – Discussion started: 16 April 2024
Revised: 1 October 2024 – Accepted: 8 October 2024 – Published: 29 November 2024

**Abstract.** For nearly 30 years, the International Network to study Deposition and Atmospheric chemistry in AFrica (INDAAF) programme has measured surface ozone from 14 sites in Africa representative of the main African ecosystems: dry savannas (Banizoumbou, Niger; Katibougou and Agoufou, Mali; Bambey and Dahra, Senegal), wet savannas (Lamto, Côte d'Ivoire; Djougou, Benin), forests (Zoétélé, Cameroon; Bomassa, Republic of the Congo) and agricultural–semi-arid savannas (Mbita, Kenya; Louis Trichardt, Amersfoort, Skukuza and Cape Point, South Africa). The data are collected with passive samplers and archived as monthly averages; quality assurance is maintained by INDAAF's calibration and intercomparison protocols with other programmes employing the same systems. This analysis reports on correlations of INDAAF ozone time series (1995–2020) with local meteorological parameters and with ozone precursors, biogenic volatile organic compounds (BVOCs) and nitrogen oxides ($NO_x$), derived from standard global databases. Mean annual averages of surface ozone range from $3.9 \pm 1.1$ ppb (Bomassa) to $30.8 \pm 8.0$ ppb (Louis Trichardt), reflecting a general positive gradient from west central Africa to South Africa. At the decade scale, from 2000 to 2020, the Katibougou and Banizoumbou sites (dry savanna) experienced a significant decrease in ozone of around $-2.4$ and $-0.8$ ppb per decade, respectively. These decreasing trends are consistent with those observed for nitrogen dioxide ($NO_2$) and BVOCs. An increasing trend is observed in Zoétélé (2001–2020), estimated at $+0.7$ ppb per decade, and at Skukuza (2000–2015; $+3.4$ ppb per decade). The increasing trends are consistent with increasing biogenic emissions at Zoétélé and $NO_2$ levels at Skukuza. Very few surface $O_3$ measurements exist in Africa, and the long-term results presented in this study are the most extensive for the ecosystems studied. The importance of maintaining long-term observations like INDAAF cannot be overstated. The data can be used to assess ozone

impacts on African crops. For the Tropospheric Ozone Assessment Report Phase II (TOAR II), they provide invaluable constraints for models of chemical and climate processes in the atmosphere.

## 1 Introduction

Ozone ($O_3$) is a greenhouse gas that is difficult to observe and quantify on a global scale due to its acute spatial variability resulting from its variable photochemical lifetime (between 20 and 25 d) (Cooper et al., 2020; Young et al., 2013). It has phytotoxic effects on key plant physiological processes that can significantly reduce the productivity of agricultural crops and ecosystems (Dufour et al., 2021; Lelieveld et al., 2015; Mills et al., 2018; Monks et al., 2015). At the local scale, its presence in high concentrations in the lower troposphere is harmful to human health, notably through irritation of the upper airways (Camredon and Aumont, 2007; Schultz et al., 2017). Ozone is a secondary air pollutant, meaning that it is not emitted directly but formed in the troposphere as a result of oxidative chemical reactions of precursor gases such as nitrogen oxides ($NO_x$), carbon monoxide (CO) and volatile organic compounds (VOCs) (Lu et al., 2019; Schultz et al., 2017). It is chemically lost by photodissociation, by surface deposition and uptake by plant stomata (Silva and Heald, 2018), or by heterogeneous reactions involving aerosols. Stomatal uptake of $O_3$ and subsequent damage to plants can lead to changes in biosphere–climate interactions (Sadiq et al., 2017). Mitigating its negative impacts on health requires reducing both pollutant concentrations and population exposure (Petetin et al., 2022). These changes are compounded by the variation in $O_3$ precursors, which in recent decades have shifted from high and middle latitudes to low latitudes, where $O_3$ production efficiency is greater (Zhang et al., 2016). These variations are particularly significant in tropical regions, where seasonal cycles linked to natural and anthropogenic sources of gas and particle emissions are well marked (Adon et al., 2010). Zhang et al. (2016) indicate that both modelling and observational studies about ozone trends are not uniform regionally or seasonally, i.e. even in the tropics where a number of sites with ozonesonde profiles exhibit no trend (Thompson et al., 2021). A study with sondes over equatorial South-East Asia by Stauffer et al. (2024) shows no definite ozone trend annually but a 6 %–8 % per decade increase limited to 3 months $yr^{-1}$. Air quality forecasts could therefore be used to warn the population of the potential occurrence of a pollution episode (Petetin et al., 2022). Its long-term importance for atmospheric chemistry has been investigated by several studies on air quality (Monks and Leigh, 2009) and on atmosphere–biosphere interactions (Fowler et al., 2009).

The International Global Atmospheric Chemistry (IGAC) project has produced the Tropospheric Ozone Assessment Report (TOAR) on the global measures for climate change, human health and crop/ecosystem research (https://igacproject.org/activities/TOAR/TOAR-II, last access: 26 November 2024). This report states that free-tropospheric $O_3$ increased during the industrial era and in recent decades (Gaudel et al., 2018; Tarasick et al., 2019). Despite these years of regional and global surface $O_3$ research and monitoring, many regions of the world such as Africa, South America, the Middle East and India remain undersampled, leading to incomplete knowledge of the horizontal, vertical and temporal distribution of $O_3$ (Cooper et al., 2014; Lin et al., 2015; Mills et al., 2018; Oltmans et al., 2013; Sofen et al., 2016). Although Africa is considered one of the continents most sensitive to air pollution and climate change, it is one of the least studied (Laakso et al., 2012; Swartz et al., 2020a).

From this perspective, long-term measurement programmes play a vital role in studies of air pollution and the various changes in the chemical composition of the atmosphere. These long-term assessments are crucial for posing the most topical research questions on atmospheric chemistry (Vet et al., 2014) in order to provide the right answers for relevant decision-making at local and global scales. In situ, satellite, ozonesonde and aircraft observations (IAGOS research infrastructure) provide a substantial amount of information on the current distribution of tropospheric $O_3$ and its variability and trends (Gaudel et al., 2018; Tarasick et al., 2019). They are well suited to improving our understanding of emissions, transport, chemical reactions and deposition processes and of the impacts of atmospheric species on human health, vegetation and climate change (Lefohn et al., 2018). Numerous long-term projects and programmes have therefore sprung up in several places around the world over several decades.

In Africa, the International Network to study Deposition and Atmospheric chemistry in AFrica (INDAAF; https://indaaf.obs-mip.fr, last access: 30 October 2024), operational since 1995, is dedicated to studying the evolution of the chemical composition of the atmosphere and deposition fluxes. INDAAF is a national observatory (Service National d'Observation, SNO) of the Institut National des Sciences de l'Univers (INSU) of the Centre National de Recherche Scientifique (CNRS) and of the Institut de Recherche pour le Développement (IRD), and it is a labelled component of the European research infrastructure ACTRIS (Aerosols, Clouds and Trace gases Research Infrastructure). The INDAAF long-term monitoring network is also labelled by the Global Atmosphere Watch Programme (GAW) of the World Meteorological Organization (WMO) as a contributing network and is a component of the DEBITS (Deposition of Bio-

geochemically Important Trace Species) activity of IGAC (International Global Atmospheric Chemistry).

Previous studies have considered surface ozone levels in Africa. Indeed, many large African international field campaigns (EXPRESSO, SAFARI-92/TRACE-A, ORACLES, SAFARI 2000, MOZAIC, Analyse Multidisciplinaire de la Mousson Africaine (AMMA)) have been performed over the past 30 years on African air quality and environment. The links to dynamical factors affecting ozone seasonality (Diab et al., 2003, 2004), the interannual variability in ozone related to El Niño–Southern Oscillation (ENSO) and $NO_x$ (Balashov et al., 2014) over the South African Highveld, regional convective influence, and the ENSO transition (Thompson et al., 2003) and the widespread impact of biomass burning and domestic fires in southern Africa occurring for several months each year are well established (Thompson et al., 2003). The mean ozone profile in the lower troposphere over the coast of the Gulf of Guinea (December–February) and over Congo (June–August) in the burning season is characterized by systematically high ozone (Sauvage et al., 2005). The combination of high $NO_x$ emissions from soil north of 13° N and northward advection by the monsoon flux of VOC-enriched air masses contributes to the ozone maximum simulated at higher latitudes (Saunois et al., 2009). Adon et al. (2010) characterized the ozone concentration levels (together with several atmospheric pollutants), from 2002 to 2007, at seven remote sites in west and central Africa, while Martins et al. (2007) investigated $O_3$ concentrations in southern Africa over a period of 9 to 11 years (1995–2005). The high ozone values recorded in southern Africa by Martins et al. (2007) are linked to the anthropogenic effect on the chemical species recorded in the atmosphere of the region. Biogenic emissions are the main contributor to ozone production, through the emission of $NO_x$ as precursors during the wet season in the dry-savanna region (Adon et al., 2010). This result is consistent with the observations made by Saunois et al. (2009) during the AMMA programme. In the dry season (wet savanna), biomass burning is the dominant factor, as mentioned by Sauvage et al. (2005). As for the tropical forests of central Africa, they appear to be a major $O_3$ sink. In South Africa, Swartz et al. (2020a) assessed long-term seasonal and interannual trends of $O_3$ based on a 21-year (1995–2015) dataset at the Cape Point station. This work was continued at three historic IDAF (IGAC–DEBITS–AFrica) sites (Amersfoort, Louis Trichardt, Skukuza; Swartz et al., 2020b). No trends of $O_3$ were observed at these four sites, and the concentrations remained relatively constant over the sampling period. The ENSO made a significant contribution to modelled $O_3$ levels at Amersfoort, Louis Trichardt and Skukuza, thus confirming the studies of Balashov et al. (2014) and Thompson et al. (2003). The influence of local and regional meteorological factors was also evident. Laban et al. (2018) reported $O_3$ levels in north-eastern South Africa and characterized the links between observed $NO_x$ and $O_3$ concentrations. These studies were completed by the effect of precursor species and meteorological conditions on ozone formation (Laban et al., 2020). The critical role of regional-scale $O_3$ precursors such as via high anthropogenic emissions of $NO_x$ (under a limited regime of VOC), coupled with meteorological conditions, is well emphasized and is in agreement with Swartz et al. (2020a, b). Further work has been carried out in different locations in Africa to characterize $O_3$ levels. The conclusions of these studies reported an increase in the tropospheric column with a mean of 1.2 nmol $mol^{-1}$ per decade (2.4 % per decade) above the Gulf of Guinea and of +3.6 % over South Africa (Bencherif et al., 2020; Gaudel et al., 2020). A strong diurnal variation in $O_3$ is observed with a maximum at midday or in the afternoon due to the local photochemical production (Hamdun and Arakaki, 2015; Ihedike et al., 2023; Khoder, 2009; Zunckel et al., 2004). The low surface ozone concentrations recorded at many sites could be caused by titration of $O_3$ by $NO_x$ (Hamdun and Arakaki, 2015; Ngoasheng et al., 2021), but the higher $NO_x$ concentrations lead to increased $O_3$ chemical production (Brown et al., 2022). The influence of local climate phenomena such as harmattan, temperature, humidity and radiation on ozone formation has also been raised (Balashov et al., 2014; Ihedike et al., 2023; Khoder, 2009). Using aircraft-based measurements of $O_3$ and a range of its precursors in African wildfire outflow over Senegalese and Ugandan savanna and over the North Atlantic Ocean near Cabo Verde, Lee et al. (2021) suggested that the contribution of biomass burning to the $O_3$ burden over the Atlantic could be underestimated. In the studies of Lannuque et al. (2021), Sauvage et al. (2007) and Tsivlidou et al. (2023), it appears clearly that tropical meteorology particularly impacts the $O_3$ distributions through the movement of air masses in the Intertropical Convergence Zone (ITCZ) due to the north-easterly harmattan flow (January) or the south-easterly winds and monsoon flow (July). Other projects such as POLCA (POLlution des Capitales Africaines) and DACCIWA (Dynamics–Aerosol–Chemistry–Cloud Interactions in West Africa) have also been implemented in African capitals such as Bamako, Dakar and Yaoundé (Adon et al., 2016) and in Abidjan and Cotonou (Bahino et al., 2018) and have provided $O_3$ concentration surface measurements. These studies confirmed that in cities where $NO_2$ is high, $O_3$ is less abundant than in rural areas, as reported in Hamdun and Arakaki (2015) and Ngoasheng et al. (2021).

However, despite many African studies about ozone and air quality, it should be noted that these campaigns, for the most part, are only snapshots in time. The number of measurements publicly available is very small, and INDAAF is among the few long-term datasets that are available to the scientific community. With the exception of South Africa, $O_3$ variability is not yet sufficiently documented, and very little information is available on the long-term evolution of $O_3$ chemistry in Africa (Fleming et al., 2018; Gaudel et al., 2018; Mills et al., 2018). Studies on the isoprene emissions changes and the temperature sensitivity of $NO_x$ and

$O_3$ chemistry (Brown et al., 2022) as well as meteorological changes involved in the seasonality and spatial patterns of ozone trends in the tropics (Stauffer et al., 2024) are therefore recommended. The impact of meteorological parameters (temperature, humidity, rainfall, radiation) and atmospheric chemistry ($NO_x$ and VOC concentrations) on the seasonality of $O_3$ concentrations, and the analysis of long-term $O_3$ trends have been only partially explained. Further work is therefore needed to fill the data gaps in Africa and better understand the mechanisms of $O_3$ formation as a function of ecosystems and their long-term evolution.

As part of the INDAAF programme, this study aims to improve the long-term assessment of surface $O_3$ in the western, central, eastern and southern African regions. For the first objective, we document the long-term (1995–2020 depending on the site) monthly, seasonal and interannual variability in $O_3$ concentrations on a regional scale at 14 sites grouped by ecosystem (dry savannas, humid savannas, forests and agricultural–semi-arid savannas), and this is followed by a comparative study with existing references. The study goes further by discussing the seasonal architecture of anthropogenic and biogenic $O_3$ precursors based on meteorological parameters and emission inventories and the correlation between $O_3$ and these factors (second objective). For the third objective, we use non-parametric statistical tests to assess long-term seasonal and annual trends in $O_3$, and we discuss the results according to trends in anthropogenic and biogenic emissions of precursors and several new trend studies that include African data. For the first time, the chemical evolution of tropospheric $O_3$ is examined over the long term at all INDAAF and companion sites. This study provides robust regional mapping of the long-term seasonal cycle $O_3$ formation at the continental scale.

## 2 Materials and methods

### 2.1 Sampling sites

Fourteen $O_3$ measurement sites located in different African ecosystems have been selected for this long-term study of tropospheric $O_3$ chemistry (Fig. 1), among which eight stations of the INDAAF long-term monitoring network are located in seven west and central Africa countries (Mali, Niger, Côte d'Ivoire, Senegal, Benin, Congo and Cameroon). These sites are characteristic of dry-savanna, wet-savanna, forest, agricultural and semi-arid ecosystems (Table 1). A detailed description of INDAAF monitoring stations and land use classes is available in Adon et al. (2010, 2013). Other sites implemented through INDAAF's companion projects and using the same $O_3$ measurements protocols were also selected for this study. The site of Dahra in Senegal, part of the Cycle de l'Azote entre la Surface et l'Atmosphère en afriQUE (CASAQUE) project, is located in dry savanna and is used for grazing (Bigaignon et al., 2020). The site of Mbita, part of the International Nitrogen Management System (INMS), is located in east Africa. In South Africa, four long-term DEBITS sites (Louis Trichardt, Skukuza, Cape Point and Amersfoort) are considered. They are regionally representative of the specific ecosystems of southern Africa. Full descriptions of these South African sites can be found in the works of Conradie et al. (2016), Laakso et al. (2012) and Swartz et al. (2020a, b). All study sites are representative of semi-natural rural sites in remote regions. Table 1 presents geographical coordinates and some ecological and climatological characteristics of the sites. In the remainder of the text, the measuring stations will be referred to using the following abbreviations: Banizoumbou (Ba), Katibougou (Ka), Agoufou (Ag), Bambey (Bb), Dahra (Da), Lamto (La), Djougou (Dj), Zoétélé (Zo), Bomassa (Bo), Mbita (Mb), Louis Trichardt (LT), Skukuza (Sk), Cape Point (CP) and Amersfoort (Af).

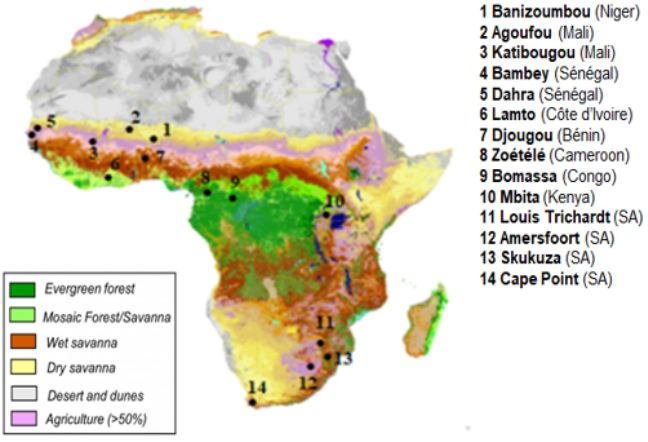


**Figure 1.** Location of the 14 measurement studied sites in Africa on a vegetation map (adapted from Mayaux et al., 2004). "SA" denotes South Africa.

### 2.2 Passive sampling and chemical analysis

#### 2.2.1 Sampling procedure

$O_3$ concentrations were measured using passive samplers developed at the Laboratoire d'Aérologie (LAERO) in Toulouse in the framework of the INDAAF programme and at the North-West University in Potchefstroom in South Africa. They are based on the passive sampling technique, which relies on laminar diffusion and the chemical reaction of the atmospheric pollutant under consideration (Adon et al., 2010; Ferm, 1991; Martins et al., 2007). These sensors have been tested and validated in different tropical and subtropical regions (Carmichael et al., 2003; Martins et al., 2007). The measurement protocols including passive sampler deployment and analysis by ionic chromatography and the calculation method of concentrations have been extensively described in previous studies (Adon et al., 2010; Bahino et al., 2018; Carmichael et al., 2003; Ferm and Rodhe, 1997; Galy-

**Table 1.** Geographical, ecological and climatic characteristics of the study sites.

| Ecosystem | Station | Latitude, longitude | Country | Land cover classes | Climate |
|---|---|---|---|---|---|
| Dry savanna | Banizoumbou (Ba) | 13°18′ N, 2°22′ E | Niger | Open grassland with sparse shrub and crops | Sahelian |
| | Katibougou (Ka) | 12°56′ N, 7°32′ W | Mali | Deciduous shrubland with sparse trees | Sudano-Sahelian |
| | Agoufou (Ag) | 15°20′ N, 1°29′ W | Mali | Open grassland with sparse shrub and trees | Sahelian |
| | Bambey (Bb) | 14°42′ N, 16°28′ W | Senegal | Cultivated grass land with sparse trees | Sahelian |
| | Dahra (Da) | 15°24′ N, 15°26′ W | Senegal | Open grassland with sparse shrub and trees, silvopastoral area | Sahelian |
| Wet savanna | Lamto (La) | 6°13′ N, 5°02′ W | Côte d'Ivoire | Mosaic forest/savanna | Guinean |
| | Djougou (Dj) | 9°39′ N, 1°44′ E | Benin | Deciduous open woodland | Sudano-Guinean |
| Forest | Zoétélé (Zo) | 3°10′ N, 11°49′ E | Cameroon | Dense evergreen lowland forest | Guinean |
| | Bomassa (Bo) | 2°12′ N, 16°20′ E | Congo | | Guinean |
| Agricultural field | Mbita (Mb) | 0°25′ S, 34°12′ E | Kenya | Tropical agricultural area | Subtropical |
| Regional savanna/ semi-arid | Louis Trichardt (LT) | 22°59′ S, 30°01′ E | South Africa | Cultivated–semi-arid regional savanna | Subtropical |
| | Skukuza (Sk) | 24°59′ S, 31°35′ E | | Semi-arid regional background site surrounded by natural bushveld in a protected area | Subtropical |
| | Cape Point (CP) | 34°21′ S, 18°29′ E | | Southern Hemispherical marine background site, rocky and sparsely vegetated, Fynbos biome | Mediterranean |
| | Amersfoort (Af) | 27°04′ S, 29°52′ E | | Semi-arid regional savanna, impacted by anthropogenic activities | Warm temperate |

Lacaux et al., 2009; Galy-Lacaux and Modi, 1998; Ossohou et al., 2019; Swartz et al., 2020b).

Sampling periods at the measurement sites were coordinated, and passive samplers were exposed on a monthly basis using the calendar months. One blank dedicated to ozone was included in the expedition of samplers every 2 months at sites. In this way, the delay between field deployment and analysis were the same for both blanks and exposed samples. All data presented in this paper were blank-corrected. A total of 1317 blanks were assessed at the 14 sites over the studied period. In this paper, we use a monthly database of $O_3$ concentrations. The concentration measurement period ran from the start date of measurements at each site to 2015–2020 (Table 2). The ozone concentration collection efficiency (%) in the sampling period (ratio of the number of valid concentrations to the number of filters analysed) was assessed at each of the 14 sites (Table 2). All wet- and dry-season durations are indicated in Table 2. These proportions are fairly representative of high-quality measurements, as indicated in the work of Laakso et al. (2008, 2012), Laban et al. (2018) and Petäjä et al. (2013). Measurements of $O_3$ concentrations are currently continuing at the most of sites and are referenced on the INDAAF website (https://indaaf.obs-mip.fr).

#### 2.2.2 Validation and quality control of INDAAF passive samplers

To ensure the reliability of the ozone concentrations measurements carried out by the passive sampling monitoring network in west, central, east and southern Africa, several validation and quality control tests were carried out as part of the IGAC–DEBITS programme and other collaborations with the Swedish Environmental Research Institute (IVL), the AMMA programme, and the pilot programme GAW Urban Research Meteorology and Environment (GURME) launched by WMO GAW and the National University of Singapore. These various performance tests were carried out in Africa at the Banizoumbou (Niger), Zoétélé (Cameroon), Lamto (Côte d'Ivoire), Djougou (Benin) and Cape Point (South Africa) sites; in France at Toulouse; and in Asia (Singapore). In this assessment, the precision and accuracy of the passive samplers used for $O_3$ monitoring by the various institutions were determined. Ozone detection limits were calculated on the basis of laboratory blank samples. Comparison of gas concentrations measured by passive samplers (integrated over 15 d) and active analysers was carried out at various sites in Toulouse (1998–2020). The test results indicated a good correlation between the two measurement methods, with an average comparative ratio of 1 : 0.8 for ozone and a correlation coefficient $R^2 = 0.8$ (Adon et al., 2010). During the 2007 AMMA campaign in Djougou, an intercomparison between measurements from passive samplers and active analysers during the wet season from April to September 2006 revealed that the maximum difference observed between the two techniques (passive and active) was around 6 % (Adon et al., 2010). In Banizoumbou, Zoétélé, Lamto and Cape Point, INDAAF and IVL passive samplers were co-located and exposed for a period of 1 year. The correlation was good between the two types of measurements (Adon et al., 2010; Carmichael et al., 2003). The most recent evaluation of the University of the North-West passive samplers used at the South African sites was an international comparison study organized by the National University of Singapore in 2008 (Swartz et al., 2020b). Results indicated that the passive sensors used and operated in INDAAF compared very well with active samplers and had better accuracies. The data quality of the analytical facilities is also ensured through participation in the World Meteorological Organization (WMO) bi-annual Laboratory Intercomparison Study (LIS) (Swartz et al., 2020a, b). The recovery of each ion in standard samples was between 95 % and 105 % (Conradie et al., 2016), and the analysed data were also subjected to the $Q$ test, with a 95 % confidence threshold, to identify, evaluate and reject outliers in the datasets (Swartz et al., 2020a). Diffusive samplers have many advantages in the field, including no need for calibration, sampling tubing, electricity or technicians, and are small, light, reusable, cost-efficient and soundless (Adon et al., 2010).

### 2.3 Meteorological parameters and the leaf area index

In order to characterize each measurement site, classical meteorological parameters are used such as relative humidity, ambient air temperature, rainfall, radiation and the leaf area index (LAI). At the Ba, Bb, La, Dj and Zo sites, the data on ambient air temperature, relative humidity and rainfall are extracted from the AMMA-CATCH database (Analyse Multidisciplinaire de la Mousson Africaine–Couplage de l'Atmosphère Tropicale et du Cycle Hydrologique; http://www.amma-catch.org/, last access: 13 October 2022) and the Observatoire de recherche en environnement "Bassins versants tropicaux expérimentaux" (SO BVET; http://bvet.obs-mip.fr/, last access: 13 October 2022) (Ossohou et al., 2019). The measuring devices used at Ka, La and Bo are described in the same work (Ossohou et al., 2019). At the Bb site, relative humidity, temperature and rainfall data are collected in the INDAAF database (https://indaaf.obs-mip.fr). At the Da site, measurements of meteorological parameters come from a measuring station installed by the University of Copenhagen (Bigaignon et al., 2020). In Ka, Ag, Bo, Mb, LT, Af, Sk and CP, the meteorological data are provided by the intermediate reanalysis archive (ERA5) of the European Centre for Medium-Range Weather Forecasts (ECMWF). The time series of global solar radiation used in this study at all sites except Dahra are also ERA5 reanalysis data obtained from ECMWF. To ensure the reliability of the ERA5 data for the study sites, we determined the estimation errors (RMSEs) and the correlation between the reanalysis data and those measured in situ. We chose the Banizoumbou site in Niger (2000–2020), which hosts a meteoro-

**Table 2.** Sampling period and concentration data collection efficiency.

| Ecosystem | Station | Sampling period | Detection limit (ppb) | Data collection efficiency (%) | Total no. of samplers | Season | Measurement altitude (m) |
|---|---|---|---|---|---|---|---|
| Dry savanna | Ba | 2000–2020 | 0.1 | 93.5 | 248 | Dry season: October–May | 1.5 |
| | Ka | 2001–2020 | | 86.7 | 240 | Wet season: June–September | |
| | Ag | 2005–2018 | | 82.6 | 132 | | |
| | Bb | 2016–2020 | | 94 | 50 | | |
| | Da | 2012–2020 | | 83.7 | 104 | | |
| Wet savanna | La | 2001–2020 | | 94.2 | 240 | Dry season: November–March | 1.5 |
| | Dj | 2005–2020 | | 92.5 | 186 | Wet season: April–October | 1.5 |
| Forest | Zo | 2001–2020 | | 86.7 | 240 | Dry season: December–February and July–August<br>Wet season: March–June and September–November | 3 |
| | Bo | 2001–2020 | | 68.3 | 240 | Dry season: December–February<br>Wet season: March–November | |
| Agricultural field | Mb | 2017–2020 | | 95.3 | 43 | Dry season: June–October and January–February<br>Wet season: March–May and November–December | 1.5 |
| Regional savanna/ semi-arid | LT | 1995–2015 | 0.02 | 95.2 | 248 | Dry season: April–September | 1.5 |
| | Sk | 2000–2015 | | 86 | 192 | Wet season: October–March | |
| | Af | 1997–2015 | | 85.5 | 221 | | |
| | CP | 1995–2020 | | 90.7 | 248 | Dry season: October–March<br>Wet season: April–September | |

logical station that provides temperature, humidity and rainfall data, and the Dahra site, where radiation data are measured. We obtained a low error estimate (RMSE) of the order of $9.9 \times 10^{-3}$ °C for temperature, $4.8 \times 10^{-3}$ % for humidity and $2.3 \times 10^{-1}$ mm for rainfall in Niger. At the Bambey site in Senegal, the estimated errors are of the order of $6.4 \times 10^{-2}$ J m$^{-2}$ for radiation. The correlation between in situ and ERA5 data for these two sites is very good: about 0.96 for rainfall, 0.99 for humidity, 0.80 for radiation and 0.99 for temperature. LAI data are obtained from MODIS (Moderate Resolution Imaging Spectroradiometer) with a resolution of 0.25 km$^2$ for an 8 d timescale centred around each station (Ossohou et al., 2019). All these parameters are collected in the same sampling period as $O_3$ concentrations, with the exception of LAI measurements, which began in 2000 (https://modis.ornl.gov/data.html, last access: 29 October 2022).

## 2.4 $NO_x$ and VOC emissions

The emissions of VOCs and $NO_x$ from biomass combustion were downloaded from the Global Fire Emissions Database Version 4 (GFED4) inventory for $0.25° \times 0.25°$ grid cells in the ECCAD (Emissions of atmospheric Compounds and Compilation of Ancillary Data) database. Biogenic VOC (BVOC) emissions are extracted from the MEGAN-MACC inventory in the ECCAD database (http://eccad.aeris-data.fr, last access: 30 November 2022). The biogenic NO fluxes used are model outputs in reference to the work of Delon et al. (2010, 2012). They were filtered in the eastern grid from 5° S to 20° N in latitude and 20° W to 30° E in longitude over the period from 2002 to 2007 and cover only the Ba, Ka, Ag, La, Dj, Zo and Bo sites. The ECCAD platform is the emissions database of the international GEIA (Global Emissions InitiAtive: http://www.geiacenter.org, last access: 26 November 2024) project, which has been developed within the framework of the French atmospheric data centre AERIS (http://www.aeris-data.fr, last access: 26 November 2024) (Darras et al., 2022). The GFED4 inventory is based on satellite data of fire activity and vegetation productivity that have been observed since 1997 (http://eccad.aeris-data.fr). The MEGAN (Model of Emissions of Gases and Aerosols from Nature) inventory quantifies net biogenic emissions of isoprene and other gases emitted by vegetation into the atmosphere (Guenther et al., 2006; Sindelarova et al., 2014). The determining variables of MEGAN are derived from models and satellite and ground observations, enabling simulations to be carried out on a regional and global scale. They take into account the emission factor, which represents the emission of a compound in the canopy under standard conditions; the emission activity factor, which includes changes in emissions due to deviations from standard conditions; and the factor that explains production and losses within the plant

canopy (Guenther et al., 2006). Isoprene, $\alpha$-pinene and $\beta$-pinene, which account for the largest proportion of BVOCs emitted by vegetation in Africa (Ferreira et al., 2010; Jaars et al., 2016; Liu et al., 2021; Saxton et al., 2007; Serça et al., 2001), were identified and used in this study. A more detailed description of these emission inventories is discussed in the work of García-Lázaro et al. (2018), Guenther et al. (2006) and Vitolo et al. (2018). For each emission category, $NO_x$ ($kg\,m^{-2}\,s^{-1}$) and VOC ($kg\,m^{-2}\,s^{-1}$), we use the sum of fluxes from all biomass combustion sources (agriculture, waste combustion, savanna, grassland, scrubland, boreal forest, temperate forest, tropical deforestation, peat degradation and peat fires) at a monthly scale and over the study period for each site. These inventory emissions are widely used, and the Global Fire Emissions Database (GFED) has been recommended by Stauffer et al. (2024) to study potential shifts in the timing and spatial patterns of biomass burning and ozone precursor emissions in the tropics.

### 2.5 Statistical analysis

The Mann–Kendall and seasonal Kendall tests, associated with the calculation of Sen's slope (Sen, 1968), are applied to all sites with at least 10 years of measurements using XLSTAT 2022.2.1 software at 95 % confidence intervals. In the case of Kendall's seasonal test, the seasonal nature of the series is taken into account. The literature provides extensive information on Mann–Kendall trend calculations (Frimpong et al., 2022; Hirsch et al., 1982; Kendall, 1975; Merabtene et al., 2016). Vectors with $p$ values of less than 0.05 exhibit a very high certainty of obtaining the trend, while vectors with $p$ values in the range of 0.05–0.10 give a medium-certainty indication of a trend (Gaudel et al., 2018). Vectors with $p$ values in the range of 0.10–0.34 provide a weak indication of change, and $p$ values greater than 0.34 indicate very weak or no change. The vectors with $p$ values in the range of 0.05–0.34 are very useful for understanding regional trends as they typically follow the same pattern as the very high certainty vectors (Chang et al., 2017; Gaudel et al., 2018). Another non-parametric breakpoint test (Pettitt test) is carried out using KhronoStat 1.01 software to assess possible breaks in homogeneity in the $O_3$ concentration series and for optimal application of the trend test.

## 3 Results and discussion

### 3.1 Meteorological and biophysical parameter variation

The monthly variations in meteorological parameters and leaf area indexes (LAI) are shown in Fig. 2 for all sites. In dry savanna, the rainfall regime is unimodal, with the greatest amounts of rain recorded from July to September corresponding to the maxima of LAI. Mean air temperature ranged from $22.1 \pm 0.9$ to $34.9 \pm 0.4$ °C, with air relative humidity from 68 % to 82 %. The most elevated solar radiation is found at Ag ($23.1 \pm 0.5\,MJ\,m^{-2}$). In wet-savanna and forest sites, the rainfall pattern and LAI follow a quasi-bimodal distribution. The mean annual LAI varies from $1.2 \pm 0.3\,m^2\,m^{-2}$ (Dj) to $4.7 \pm 0.7\,m^2\,m^{-2}$ (Bo). The most significant monthly variations in relative humidity are found in Dj (23.2 %–84.1 %). At the Mb site, the maximum rainfall occurs between March and May, reaching 255 mm in April. The vegetation cover is denser at the end of the first wet season ($1.3 \pm 0.3\,m^2\,m^{-2}$ in May), with an average value of humidity of around 70 %. In southern Africa, the humidity varies from 13 % to 22 % year-round except at CP, where variations are very low. The maximum of rain is collected between December and January (432 mm on average) at the LT, Af and Sk sites and in August at CP (343 mm). LAI maxima are of the order of $1.6 \pm 0.2\,m^2\,m^{-2}$ at Af, $3.1 \pm 0.6\,m^2\,m^{-2}$ at LT, $4.0 \pm 0.1\,m^2\,m^{-2}$ at CP and $1.7 \pm 0.2\,m^2\,m^{-2}$ at Sk in the wet season. In wet savanna and forest, as well as in Mb, the temperature variations are low ($23.6 \pm 0.5$ °C). On the other hand, at the South African sites, the temperature reaches amplitudes ranging from 6 to 10 °C. From wet savanna to semi-arid savanna (South Africa), the average solar radiation is below $22\,MJ\,m^{-2}$. Along the north–south transect for the study sites, the gradients of humidity, leaf area index and rainfall are positive, whereas they are negative for temperature and radiation. The variations in meteorological parameters are strongly influenced by the alternating seasons. These characteristics are dependent on the type of climate. Indeed, in west and central Africa, climate (as well as its variability) is a function of the position of the ITCZ, which is a band separating the hot and dry continental air coming from the Sahara (harmattan) from the cooler, humid maritime air masses (monsoon) originating in the equatorial Atlantic Ocean (Adon et al., 2010; Lannuque et al., 2021; Sauvage et al., 2005). The ITCZ's geographical shift from the Northern Hemisphere during the boreal summer to the Southern Hemisphere during the boreal winter, with different positions throughout the year (for example around 5° N in January and around 22° N in August) defines the seasons in this region of Africa and explains the marked seasonal variations observed in west and central Africa (Sauvage et al., 2005). The position of the convergence zone gives rise to the "wet" seasons. Compared with west Africa, east Africa exhibits slightly different regimes due to the topography and the proximity of the Indian Ocean. The climate of southern Africa is characterized by alternating wet and dry periods, which are also modified by the position of the ITCZ (Lannuque et al., 2021). Within the ITCZ, warm and humid surface air masses converge and are convectively uplifted into the upper troposphere. The uplifted air masses are then advected polewards in the upper branches of the Hadley cells. The dry air in the descending branches of these cells creates the conditions for wildfires and the resulting emission of ozone precursors (Lannuque et al., 2021).

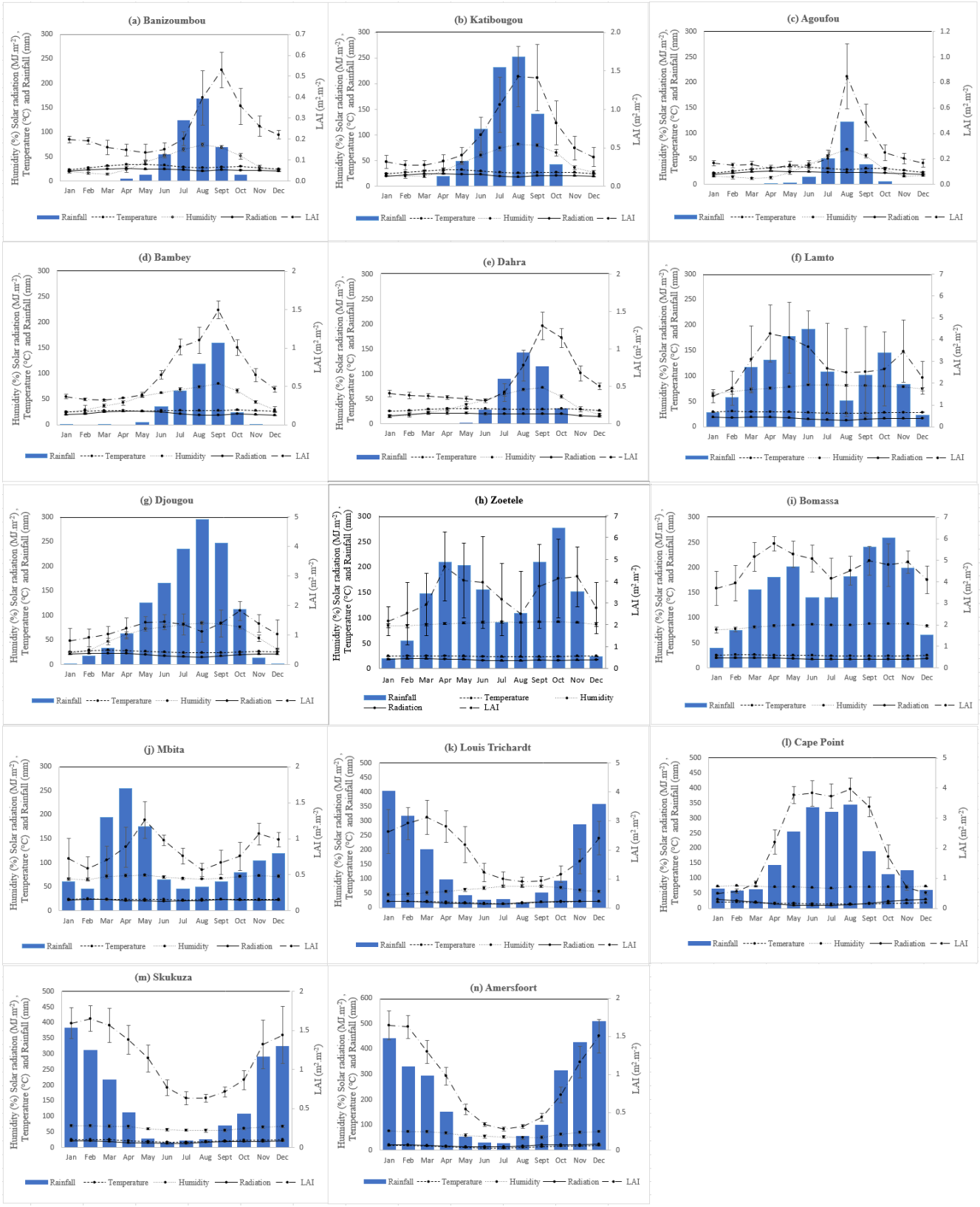


**Figure 2.** Mean monthly variation in air temperature (°C), rainfall (mm), relative humidity (%), solar radiation (MJ $m^{-2}$) and leaf area index ($m^2$ $m^{-2}$). The mean absolute deviation is represented by the vertical bars.

### 3.2 Characterization of $O_3$ levels

#### 3.2.1 Seasonal and annual variation in $O_3$ levels

##### Dry savanna

Figure 3 presents monthly $O_3$ surface concentrations measured in Ba, Ka and Ag (Fig. 3a) and Bb and Da (Fig. 3b), representative of dry savannas in Niger, Mali and Senegal. The seasonal variability in $O_3$ is well marked: $O_3$ levels during the wet season are higher than in the dry season (Table 3). At most sites, from January to May, the $O_3$ concentrations gradually increase to finally reach annual peaks at the start of the wet season (May–June–July). The mean annual cycle of monthly $O_3$ concentrations at Ba, Ka and Ag (Fig. 4a) and at Bb and Da (Fig. 4b) are obtained from averages of monthly in situ measurements over the whole studied period. The annual distribution is similar to the regional rainfall pattern. Ozone concentrations decrease as the rainy season progresses but remain at higher levels compared to the dry season. At dry-savanna sites, monthly average surface $O_3$ concentrations range from $6.1 \pm 2.4$ to $14.5 \pm 2.6$ ppb during the dry season and from $13.9 \pm 5.1$ to $19.4 \pm 3.9$ ppb during the rainy season (Table 3). From the dry to the wet season, $O_3$ levels increased from 18.7 % to 68.5 %. The annual $O_3$ concentrations ranged from $10.5 \pm 5.4$ ppb at Ka to $14.8 \pm 4.3$ ppb at Bb (Table 3).

The high $O_3$ concentrations observed at the start of the rainy season are due to soil humidification, which generates biogenic NO emissions pulses in the region, during this period. Indeed, the accumulated nitrogen in soils (in the form of ammonium and nitrate ions) from traditional agricultural practices, such as grazing, manure spreading and the decomposition of crop residues (Delon et al., 2015; Laville et al., 2005), is released into the atmosphere when the first rains fall on dry soils. Bacterial nitrification is thus activated, leading to nitrogen consumption and the consequent release of large pulses of NO (Adon et al., 2010; Delon et al., 2015; Jaegle et al., 2004; Laville et al., 2005; Ludwig et al., 2001; Ossohou et al., 2019). During the wet season, the decrease in $O_3$ levels may be attributed to a decrease in $NO_x$ concentrations. Indeed, soil mineral N is used by plants during their root growth phase and is therefore less available for the production of NO to be released into the atmosphere (Homyak et al., 2014). In Fig. 5, which presents the monthly variation in $NO_x$ and VOCs (natural and anthropogenic emissions) in dry savanna, biogenic NO fluxes (Fig. 5e, f and g) show a bell-shaped variation, peaking in August (wet season). We observe a good dependence of $O_3$ on NO ($0.73 < r < 0.92$) at Ba, Ka and Ag in the presence of high relative humidity and precipitation ($0.64 < r < 0.95$) (Table 4), that is, agreement with the high values of $O_3$ observed in the wet season over these sites. The monthly profile of BVOC fluxes (isoprene, $\alpha$-pinene and $\beta$-pinene) in dry savanna (Fig. 5) shows a maximum at the end of the dry season–beginning of wet season at Ba, Ka and Ag (Fig. 5e, f and g), or during the wet season at Bb and Da (Fig. 5h and i). Isoprene fluxes are more obvious at Da ($(214.2 \pm 30)$ ng m$^{-2}$ s$^{-1}$), whereas $\alpha$-pinene and $\beta$-pinene exhibit larger values at the Ka site ($11.2 \pm 1.8$ and $5.2 \pm 0.8$ ng m$^{-2}$ s$^{-1}$, respectively). The fluxes of $\beta$-pinene ($0.70 < r < 0.79$) and isoprene ($r = 0.79$) correlate well with $O_3$ at (1) Ba, Ka and Ag and (2) Bb and Da, respectively, under the influence of the humidity and rainfall in Mali and Niger and the temperature, radiation and humidity ($0.50 < r < 0.76$) in Senegal (Table 4).

These observations in dry savanna are confirmed by Stewart et al. (2008), who correlated $O_3$ production in the Sahel during the wet season with high $NO_x$ concentrations attributed to biogenic emissions during the AMMA campaign. In the dry savanna, Oluleye and Okogbue (2013) estimated that rain was responsible for 62 % of the $O_3$ distribution in the west African region, excluding the precursors NO, CO and hydrocarbons, as also illustrated in our results. Saunois et al. (2009) have shown that soil $NO_x$ emissions, combined with the northward advection of volatile organic compounds (VOCs), play a key role in $O_3$ production in dry-savanna regions. This large-scale impact of biogenic emissions has also been verified by Williams et al. (2009), who estimate that 2 %–45 % of tropospheric $O_3$ over equatorial Africa may originate from $NO_x$ emissions from African soils. All these works are in agreement with the results of this study. Monthly variation in anthropogenic $NO_x$ and VOC emissions (Fig. 5a, b, c and d) indicates that during the wet season, $NO_x$ and VOC fluxes are very low. On the other hand, maxima are observed in the dry season, with the highest emissions found in Ka, and could be the cause of ozone production in the dry season. Indeed, the monthly averaged biomass combustion emissions (GFED4) over an 18-year period (1998–2015) in the Sahel show that Ka is significantly affected by the biomass combustion source in November (Ossohou et al., 2019).

##### Wet savanna and forest

Figure 6 presents the mean monthly surface $O_3$ concentrations in Dj and La (Fig. 6a) and Zo and Bo (Fig. 6b). Ozone concentrations present a pattern of seasonality during the year. The maximum of the data series in La is 20.6 ppb in March (dry season), and the minimum is 4.3 ppb in October (wet season). In Dj, the $O_3$ levels are higher than in La. The highest monthly value recorded in Dj is 24.8 ppb in April (start of the wet season). At the forest ecosystem sites, $O_3$ concentrations are lower than in dry, wet and agricultural–semi-arid savannas (Table 3). In Zo and Bo, the highest annual peaks are found in February (11.1 and 8.3 ppb, respectively). Monthly averages in the dry season ranged from $4.7 \pm 1.4$ ppb (Bo) to $14.1 \pm 4.0$ ppb (Dj), and in the wet season they ranged from $3.7 \pm 1.0$ ppb (Bo) to $13.2 \pm 2.8$ ppb (Dj) (Table 3). The ozone mean annual cycle is shown in Fig. 7.

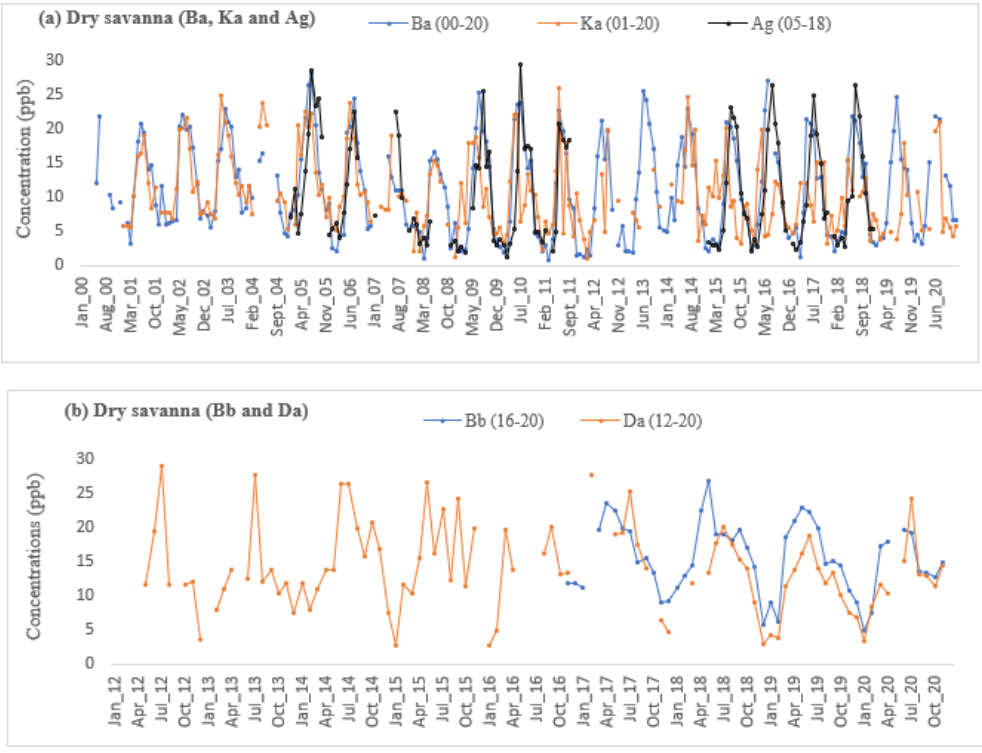


**Figure 3.** Monthly evolution of $O_3$ concentrations (ppb) in dry savanna at **(a)** Ba (Niger) and Ka and Ag (Mali) and **(b)** Bb and Da (Senegal). The numbers in parentheses after the site abbreviations denote the years when data were measured (e.g. 00–20 indicates 2000–2020; here and in similar figures).

**Table 3.** Minimum, maximum and average of monthly, annual and seasonal $O_3$ concentrations at all sites (1995–2020).

| Ecosystem | | Monthly | | Annual | Dry season | | | Wet season | | |
|---|---|---|---|---|---|---|---|---|---|---|
| | | Min | Max | Avg | Min | Max | Avg | Min | Max | Avg |
| Dry savanna | Ba | 0.9 | 28.3 | 11.2 ± 6.9 | 4.2 ± 2.7 | 16.9 ± 3.7 | 7.6 ± 2.9 | 13.6 ± 2.5 | 21.2 ± 3.5 | 18.3 ± 3.2 |
| | Ka | 1.2 | 26.1 | 10.5 ± 5.4 | 5.8 ± 2.6 | 14.9 ± 6.6 | 8.8 ± 3.7 | 11.3 ± 3.8 | 17.7 ± 5.4 | 13.9 ± 5.1 |
| | Ag | 1.4 | 29.5 | 10.5 ± 7.3 | 3.3 ± 1.1 | 12.9 ± 4.6 | 6.1 ± 2.4 | 16.4 ± 3.8 | 23.7 ± 4.6 | 19.4 ± 3.9 |
| | Bb | 4.96 | 26.7 | 14.8 ± 4.3 | 8.8 ± 3.5 | 24.0 ± 2.4 | 14.5 ± 2.6 | 15.4 ± 1.9 | 20.2 ± 1.4 | 17.7 ± 1.6 |
| | Da | 2.8 | 29.0 | 13.9 ± 6.3 | 5.0 ± 3.8 | 16.7 ± 5.4 | 11.1 ± 4.0 | 14.7 ± 3.1 | 23.7 ± 4.8 | 18.2 ± 4.0 |
| Wet savanna | La | 4.25 | 20.6 | 10.8 ± 3.3 | 9.9 ± 1.4 | 15.1 ± 2.3 | 13.5 ± 2.3 | 6.7 ± 1.1 | 12.2 ± 1.9 | 9.0 ± 1.5 |
| | Dj | 3.3 | 24.8 | 13.5 ± 4.8 | 10.8 ± 4.5 | 18.7 ± 2.7 | 14.1 ± 4.0 | 9.0 ± 2.0 | 18.4 ± 2.4 | 13.2 ± 2.8 |
| Forest | Zo | 1.2 | 11.1 | 5.2 ± 2.1 | 7.1 ± 2.1 | 7.8 ± 1.6 | 7.5 ± 2.1 | 3.5 ± 1.3 | 6.6 ± 1.9 | 4.6±1.6 |
| | Bo | 1.5 | 8.3 | 3.9 ± 1.1 | 4.0 ± 1.0 | 5.2 ± 1.2 | 4.7 ± 1.4 | 2.8 ± 1.0 | 5.4 ± 1.0 | 3.7 ± 1.0 |
| Agricultural or semi-arid savanna | Mb | 10.5 | 30.2 | 19.9 ± 4.7 | 13.8 ± 3.4 | 25.7 ± 5.7 | 20.9 ± 4.0 | 14.1 ± 5.0 | 22.5 ± 2.7 | 18.5 ± 3.9 |
| | Sk | 6.3 | 64.1 | 22.8 ± 7.3 | 23.0 ± 9.6 | 30.2 ± 6.0 | 25.9 ± 7.3 | 14.5 ± 1.9 | 29.2 ± 5.6 | 20.3 ± 5.4 |
| | Af | 3.2 | 55.5 | 26.9 ± 6.3 | 19.9 ± 6.2 | 31.2 ± 7.6 | 24.5 ± 6.3 | 23.8 ± 4.9 | 34.4 ± 7.4 | 29.0 ± 7.3 |
| | CP | 3.3 | 67.4 | 26.8 ± 6.2 | 17.3 ± 5.3 | 30.4 ± 6.0 | 23.4 ± 5.6 | 25.9 ± 6.3 | 32.1 ± 5.7 | 29.8 ± 6.1 |
| | LT | 9.0 | 86.6 | 30.8 ± 8.0 | 24.7 ± 7.9 | 40.1 ± 10.8 | 32.0 ± 8.9 | 21.3 ± 5.2 | 36.0 ± 9.1 | 28.3 ± 8.2 |

The high $O_3$ concentrations in the dry season in these two ecosystems could be related to the biomass burning source, which is generally recorded during the months of December–February in rural tropical environments, and BVOC emissions. Indeed, in wet savannas (La, Dj) and forest (Zo) (Fig. 8), $NO_x$ and VOC anthropogenic fluxes reach their maxima during the dry season. The mean flux estimates are 14.5, 24.2 and 4.9 ng $m^{-2}$ $s^{-1}$ for $NO_x$ and 26.8, 29.4 and 5.5 ng $m^{-2}$ $s^{-1}$ for anthropogenic VOCs at La, Dj and Zo (Fig. 8a, b and c), respectively. BVOC maximum fluxes are

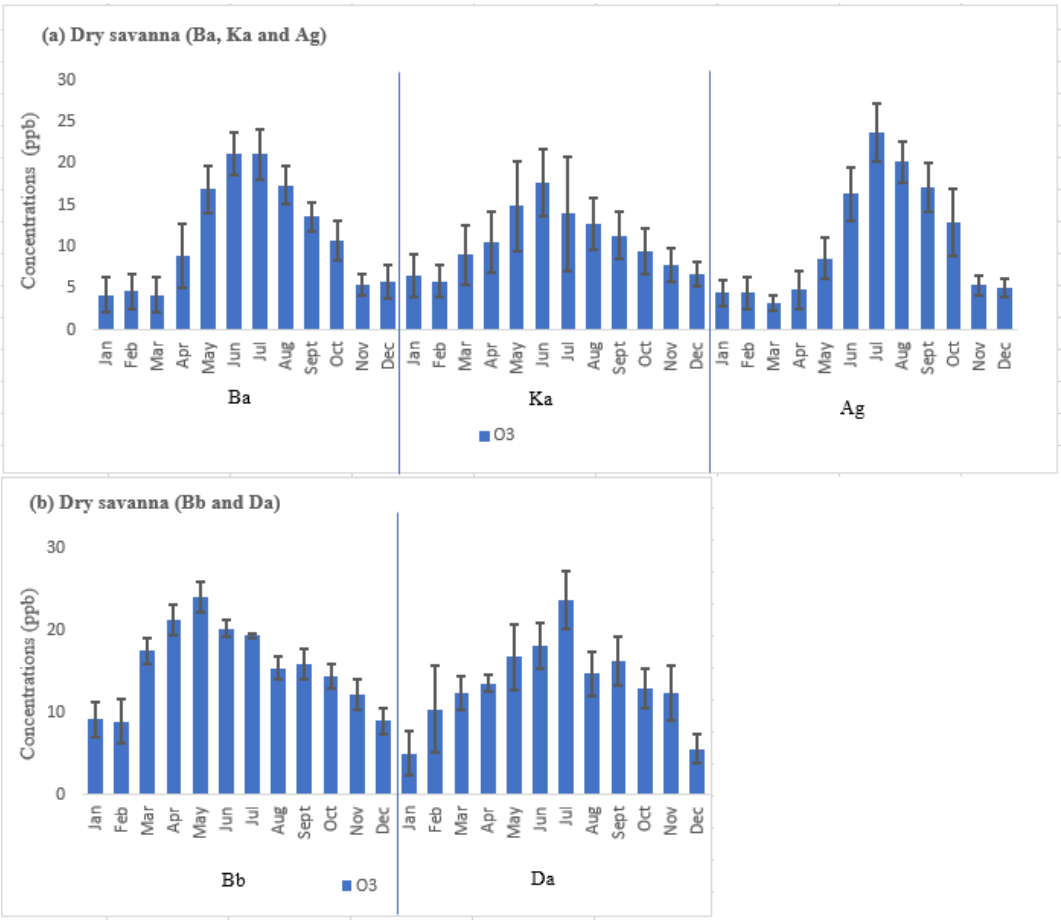


**Figure 4.** Mean monthly averages of $O_3$ concentrations (ppb) in dry savanna at **(a)** Ba (Niger) and Ka and Ag (Mali) and **(b)** Bb and Da (Senegal). Mean monthly averages are calculated from the long ozone data series of Fig. 3. Bars represent mean absolute deviation.

**Table 4.** Correlation $r$ between $O_3$ and its precursors and meteorological variables at different sites. Dashes (–) in the table indicate the absence of data at the respective site for the precursor concerned over the study period.

| Ecosystem | Dry savanna | | | | | Wet savanna | | Forest | | Agricultural–semi-arid savanna | | | | |
|---|---|---|---|---|---|---|---|---|---|---|---|---|---|---|
| Sites | Ba | Ka | Ag | Bb | Da | La | Dj | Zo | Bo | Mb | LT | CP | Af | Sk |
| | | | | | | | $O_3$ | | | | | | | |
| NO biogenic | 0.85 | 0.73 | 0.92 | – | – | −0.15 | −0.24 | −0.43 | $-10^{-3}$ | – | – | – | – | – |
| $NO_{x_{Combustion}}$ | −0.33 | −0.43 | 0.04 | – | 0.001 | 0.49 | 0.059 | 0.80 | −0.33 | 0.31 | 0.37 | −0.67 | 0.62 | 0.61 |
| $VOC_{Combustion}$ | −0.40 | −0.47 | −0.003 | – | $-5 \times 10^{-4}$ | 0.54 | 0.05 | 0.79 | −0.40 | 0.31 | 0.60 | −0.87 | 0.52 | 0.65 |
| Isoprene | 0.51 | 0.54 | 0.46 | 0.79 | 0.78 | 0.92 | 0.81 | 0.80 | 0.92 | 0.42 | −0.39 | −0.91 | 0.29 | −0.64 |
| $\alpha$-Pinene | 0.67 | 0.76 | 0.66 | 0.45 | 0.77 | 0.74 | 0.64 | 0.63 | 0.90 | 0.36 | −0.45 | −0.86 | 0.29 | −0.67 |
| $\beta$-Pinene | 0.70 | 0.79 | 0.72 | 0.34 | 0.72 | 0.70 | 0.56 | 0.60 | 0.89 | 0.33 | −0.48 | −0.85 | 0.27 | −0.71 |
| Temperature | 0.45 | 0.47 | 0.42 | 0.51 | 0.76 | 0.72 | 0.69 | 0.68 | 0.89 | 0.47 | −0.46 | −0.90 | 0.49 | −0.62 |
| Humidity | 0.82 | 0.64 | 0.95 | 0.52 | 0.70 | −0.85 | −0.19 | −0.89 | −0.79 | −0.61 | −0.79 | −0.68 | 0.1 | −0.80 |
| Rainfall | 0.74 | 0.64 | 0.75 | 0.15 | 0.51 | −0.48 | −0.39 | −0.76 | −0.54 | −0.18 | −0.49 | 0.74 | 0.53 | −0.69 |
| Radiation | 0.16 | 0.15 | 0.26 | 0.75 | 0.69 | 0.73 | 0.54 | 0.65 | 0.87 | 0.21 | −0.19 | −0.76 | 0.71 | −0.43 |

obtained at the end of the dry season–beginning of the wet season (Fig. 8e, f, g and h). A drop in these fluxes is then observed during the wet season. Strong Pearson correlations are observed between $O_3$, $NO_x$ and the VOCs ($0.49 < r < 0.92$) (Table 4). Temperature and radiation are also well correlated with $O_3$ ($0.54 < r < 0.89$) in these two ecosystems. These results are corroborated by the literature. Indeed, radiation and humidity facilitate the propagation of radical chain reactions and the production of hydroxyl radicals (OH) at these sites (Graedel and Crutzen, 1993). According to several au-

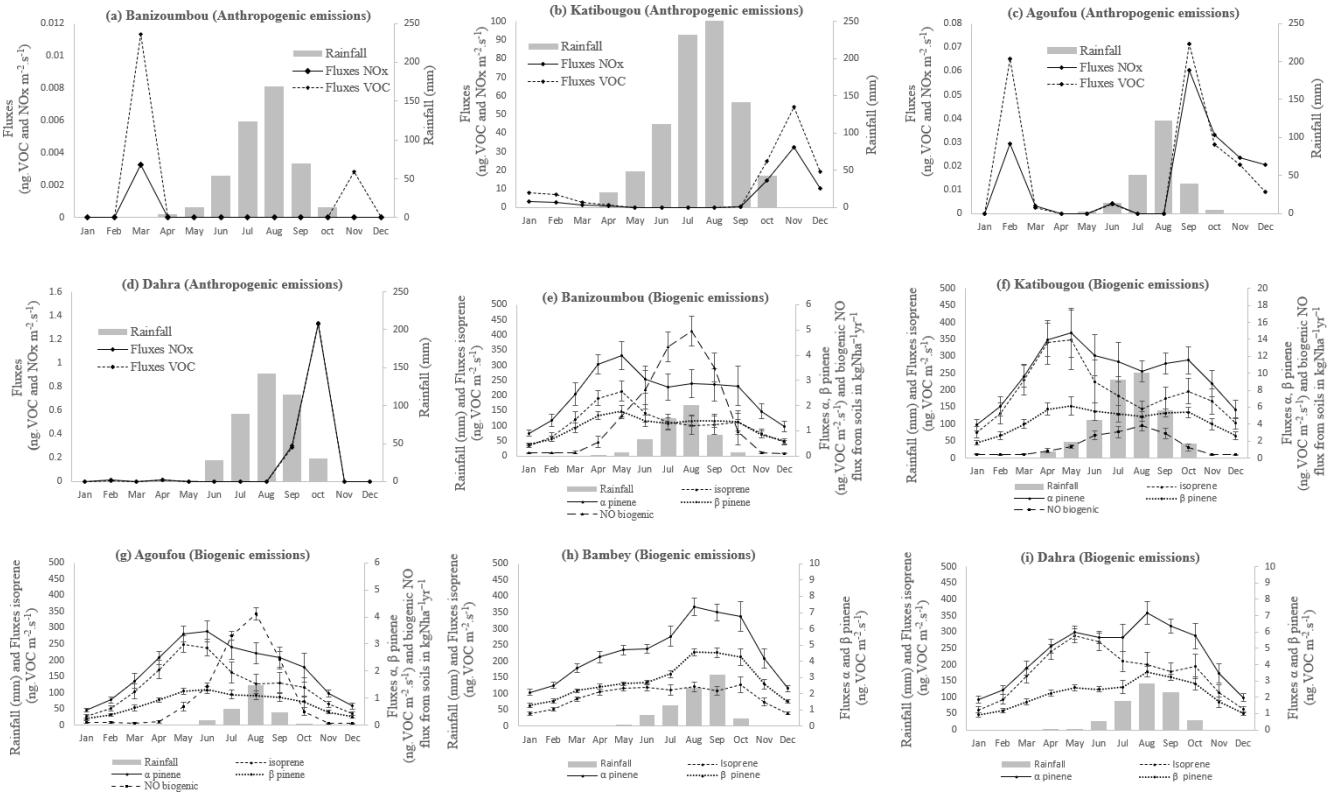


**Figure 5.** Mean monthly fluxes of natural and anthropogenic $NO_x$ and VOCs estimated by the GFED4 and MEGAN inventories for $0.25° \times 0.25°$ grid cells centred on each of the dry-savanna sites.

thors, $O_3$ levels tend to increase under warm, sunny conditions favourable to photochemical $O_3$ production (Hamdun and Arakaki, 2015; Morakinyo et al., 2020). Moreover, Aghedo et al. (2007), Mari et al. (2011), Saunois et al. (2009) and Saxton et al. (2007) have reported that vegetated areas emit large quantities of biogenic organic compounds that influence $O_3$ production in the presence of light and temperature. Others authors such as Abbadie (2006), Adon et al. (2010), Galanter et al. (2000) and Tsivlidou et al. (2023) have linked the high $O_3$ concentrations recorded in the dry season to the presence of $NO_x$ emitted by biomass combustion in the wet savanna (Gulf of Guinea). According to Adon et al. (2010), Baldy et al. (1996), Clain et al. (2009), Cros et al. (1992), Hamdun and Arakaki (2015), Martins et al. (2007), and Oluleye and Okogbue (2013), the biomass burning is likely to contribute significantly to $O_3$ production through precursor emissions ($NO_x$ and CO) in the dry season (wet savanna) with nearly 30 % to 80 % of the savanna ground surface burned annually between December and February. The high $O_3$ concentrations measured in Tharangambadi (formerly Tranquebar, India) have been linked to increased emissions of $NO_x$ and other precursors from various sources (Debaje et al., 2003). Compared to wet and dry savannas, forest sites recorded the lowest $O_3$ amounts due to significant dry deposition of $O_3$ on the ground and on foliage and trees (Mari et al., 2011; Rummel et al., 2007; Saunois et al., 2009). Tropical forests are shown to be important $O_3$ sinks. A strong gradient of $O_3$ between forest and dry savanna in west Africa has been observed from aircraft measurements (Saunois et al., 2009).

In Bo, high $NO_x$ and VOC fluxes are observed in the wet season (Fig. 8d), unlike in Zo (Fig. 8c), and this is corroborated by Ossohou et al. (2019) over the period 1998–2015. The source of these recorded anthropogenic emissions during this period of the year at Bo could be biomass combustion. According to the work of Sauvage et al. (2005), the period from August to September corresponds to a peak in biomass burning activity in the southern African countries (Mozambique, Zimbabwe, South Africa). Moving air masses over central Africa via the northern edge of the continental anticyclone could explain such high emissions at Bo in August–September.

## Agricultural and semi-arid savanna

Figure 9 presents the monthly evolution of surface $O_3$ concentration in the agricultural site (Mb) and semi-arid-savanna sites (LT, CP, Sk and Af). At the Mb site, monthly $O_3$ concentrations do not exceed 30.2 ppb (Table 3). At the CP, LT, Sk and Af sites, $O_3$ levels are almost twice as high as in west

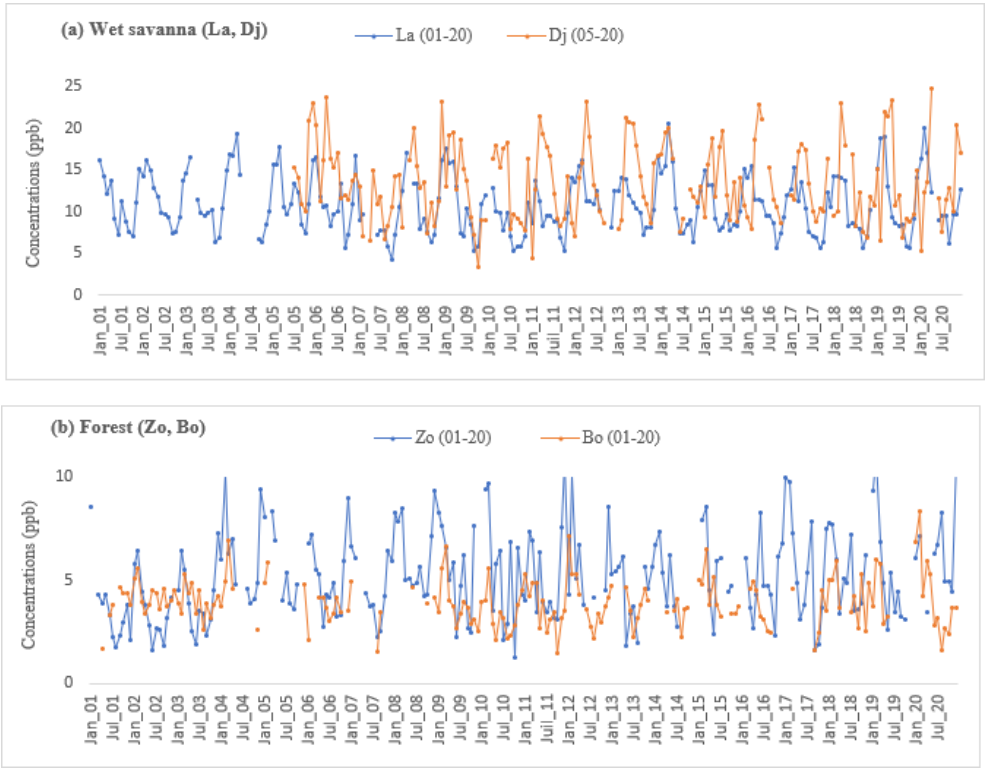


**Figure 6.** Monthly evolution of $O_3$ concentrations (ppb) in **(a)** humid savanna at La (Côte d'Ivoire) and Dj (Benin) and **(b)** forest at Zo (Cameroon) and Bo (Congo).

African sites. The mean annual cycle of $O_3$ concentrations (Fig. 10a and b) shows that at Mb, $O_3$ levels are quite similar between seasons (Table 3). In southern African ecosystems, dry-season $O_3$ concentrations are the highest at LT and Sk. The annual averages are around $19.9 \pm 4.7$ ppb at Mb, $22.8 \pm 7.3$ ppb at Sk, $26.9 \pm 6.3$ ppb at Af, $26.8 \pm 6.2$ ppb at CP and $30.8 \pm 8.0$ ppb at LT (Table 3).

These $O_3$ levels observed could be associated with the combustion sources and natural emissions. Indeed, in Fig. 11a, we observe $NO_x$ and VOC fluxes that are quantifiable in February (dry season) at Mbita. Based on the analysis of burned surface areas, Bakayoko et al. (2021) indicated that Mb is strongly influenced by biomass burning from northern and southern sides during both dry seasons. High $O_3$ levels measured at Mb site during the dry season show values similar to those in Nairobi, Kenya, during the same months (Kimayu et al., 2017). At the South African sites, Fig. 11b, c, d and e show that the mean fluxes of anthropogenic emissions vary from 0.3 ng $m^{-2}$ $s^{-1}$ (LT) to 10.2 ng $m^{-2}$ $s^{-1}$ (Sk) for $NO_x$ and from 2.9 ng $m^{-2}$ $s^{-1}$ to 11.8 ng $m^{-2}$ $s^{-1}$ (Sk) for VOCs with the maxima recorded in the dry season. As for the BVOC emissions (Fig. 11g, i and j), more specifically at LT, Af and Sk, the highest values are reached in the wet season. At CP (Fig. 11h), the maximum emissions are measured in the dry months of January and February. The calculations of correlation indicate ozone is linked to anthropogenic combustion sources at LT, Af and Sk and are anti-correlated with temperature, humidity and radiation ($-0.90 < r < -0.43$) at LT, CP and Sk (Table 4). High $O_3$ concentrations are therefore measured at these sites during the driest and coldest months (Swartz et al., 2020b). Except at Af where $O_3$ has a weak link with BVOCs, the increase in isoprene, $\alpha$-pinene, and $\beta$-pinene emissions rates is positively correlated with $O_3$ decrease at the other sites. At the CP and Af sites, rainfall and $O_3$ are correlated ($0.53 < r < 0.74$), and ozone production could therefore also be linked to microbial activity of soils at these two sites. At the CP site during the same study period, Swartz et al. (2020b) emphasized that higher $NO_2$ concentrations were attributed to increased microbial activity in the wet season and that the $O_3$ seasonal pattern corresponded to the $NO_2$ seasonality, which was attributed to their related chemistry. The importance of humidity and temperature in $O_3$ photochemistry observed at almost all South African sites has been highlighted by Balashov et al. (2014) and Laban et al. (2018, 2020).

At southern African sites, $O_3$ levels could also be attributed to a combination of regional and local influences, including emissions from industrial, vehicular and domestic biomass combustion and biomass combustion emissions in sub-Saharan Africa (Mozambique, Zambia, Zimbabwe and Angola) that are recirculated by anticyclonic air mass processes (Baldy et al., 1996; Laban et al., 2018; Martins et

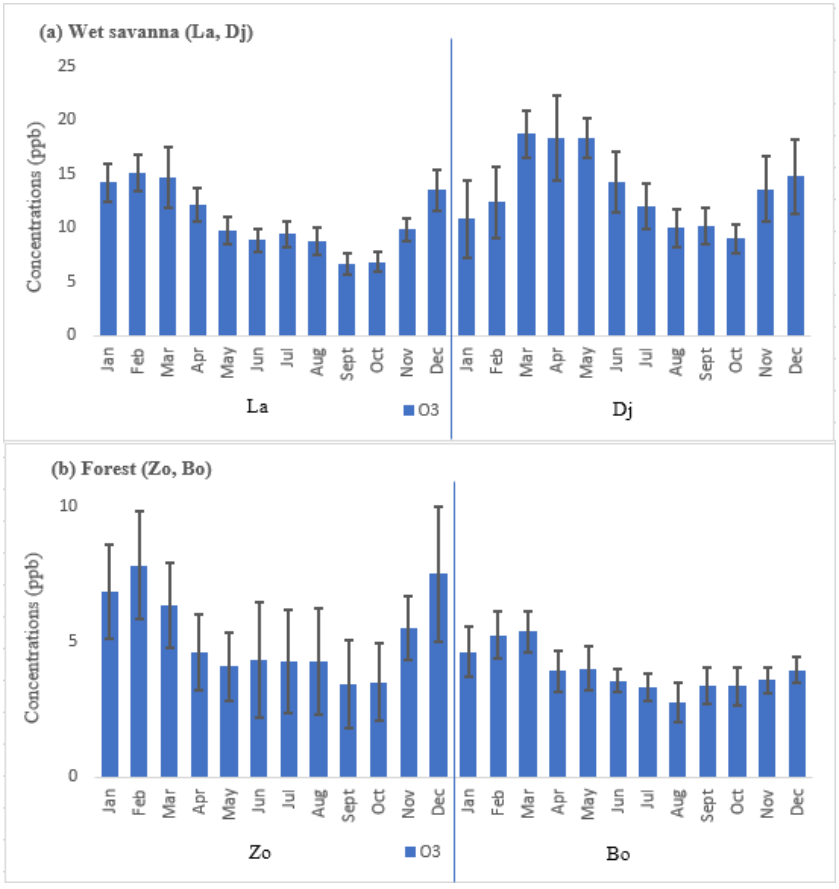


**Figure 7.** Mean monthly averages of $O_3$ concentrations (ppb) in **(a)** humid savanna at La (Côte d'Ivoire) and Dj (Benin) and **(b)** forest at Zo (Cameroon) and Bo (Congo). Mean monthly averages are calculated from the long ozone data series of Fig. 6. Bars represent mean absolute deviation.

al., 2007; Swap et al., 2003; Tiitta et al., 2014; Josipovic et al., 2010). Biomass combustion is considered a major source of $O_3$ precursors in South Africa (Ngoasheng et al., 2021; Vakkari et al., 2013) and in southern Africa (Heue et al., 2016) and may explain the $O_3$ levels observed in the dry season at LT and Sk. The high $O_3$ levels in the wet season (at Af and CP) due to soil microbial activity (Swartz et al., 2020a) could also be explained by the long-range transport of air pollutants emitted from the industrialized Highveld region (Abiodun et al., 2014; Ojumu, 2013). During the austral winter, $O_3$ concentrations in the boundary layer are higher (e.g. at CP and Af) due to a systematic increase in $O_3$ precursors from households and combustion for space heating (Bencherif et al., 2020; Laban et al., 2018; Lourens et al., 2011; Oltmans et al., 2013; Swartz et al., 2020b). The high concentrations measured at Af could also be due to industrial activities located near this site (Lourens et al., 2011).

### 3.2.2 $O_3$ levels in Africa, set in a global context

Ozone concentrations measured at the 14 sites studied are mapped on a seasonal and annual scale (Fig. 12).

We compared African ozone levels reported in this study with studies carried out in Africa and around the world over the last 20 years (Table 5, Fig. 13). The bibliographical synthesis takes into account studies where the data measurement methodology has been clearly described. Sites where concentrations have been measured by passive samplers are listed. We have identified, among others, sites in North America, north-eastern Europe, Asia and Africa. Figure 13 focuses more on $O_3$ monitoring studies in Africa.

Several sites reported in Table 5 and Fig. 13 are exposed to high $O_3$ concentrations. These different levels observed in Africa and around the world are in most cases above values reported in this study, with the exception of sites in southern Africa.

Indeed, the earlier studies have mentioned high ozone concentrations measured in southern Africa particularly. Laban et al. (2018) have observed the elevated surface ozone ($O_3$) concentrations over four sites in South Africa (Botsalano (2006–2008), Marikana (2008–2010), Welgegund (2010–2015) and Elandsfontein (2009–2010)), with an annual mean ranging from around 5 to 70 ppb. The temporal $O_3$ patterns

**Table 5.** $O_3$ concentrations at various sites worldwide as reported in the literature.

| Site | Type | Period | $O_3$ (ppb) | Reference |
|---|---|---|---|---|
| India, Tharangambadi | Rural | May 1997–October 2000 | $17 \pm 7$ to $23 \pm 9$ | Debaje et al. (2003) |
| Sweden, Malmö (20 sites) | Rural<br>Urban<br>Traffic | 16–24 April 2012,<br>28 May–4 June,<br>20–27 August 2012 | $37.0 \pm 5.4$<br>$35.0 \pm 3.9$<br>$33.6 \pm 3.5$ | Hagenbjörk et al. (2017) |
| Sweden, Umeå (20 sites) | Rural<br>Urban<br>Traffic | | $27.7 \pm 8.4$<br>$26.7 \pm 7.3$<br>$25.2 \pm 6.9$ | |
| China, Mt Waliguan | Rural | September 1999– | 44.9 | Carmichael et al. (2003) |
| Taiwan, Shuili | Rural | May 2001 | 25.0 | |
| Malaysia, Tanah Rata | Rural | | 16.0 | |
| Indonesia, Bukit Kototabang | Rural | | 10.7 | |
| India, Agra | Rural | | 30.8 | |
| Argentina, Isla Redonda | Rural | | 15.9 | |
| Brazil, Arembepe | Rural | | 19.2 | |
| Türkiye, Çamkoru | Rural | | 35.4 | |
| United Arab Emirates, Al Ain | Rural<br>Industrial<br>Traffic<br>Commercial<br>Residential | April 2005–April 2006 | 8.7<br>5.9<br>4.4<br>5.9<br>7.3 | Salem et al. (2009) |
| American Samoa, Tutuila | Urban and rural | 1990–2015 | $13.7 \pm 1.0$ | Lu et al. (2019) |
| Chile, Cerro Tololo | | | $32.0 \pm 1.3$ | |
| South Africa, Cape Point | | | $24.3 \pm 1.1$ | |
| Australia, Cape Grim | | | $24.9 \pm 0.8$ | |
| Aotearoa / New Zealand, Ōrua-pouanui / Baring Head | | | $21.4 \pm 1.6$ | |
| Syowa | | | $25.2 \pm 0.9$ | |
| Neumayer Station III | | | $24.3 \pm 1.5$ | |
| Arrival Heights | | | $25.9 \pm 1.5$ | |
| South Pole | | | $28.4 \pm 1.7$ | |
| Barrow Atmospheric Baseline Observatory | Remote | 1973–2015 | 15–44 | Cooper et al. (2020) |
| Mauna Loa Observatory (MLO) | Remote | 1973–2015 | 26–65 | |
| American Samoa Observatory | Remote | 1973–2015 | 5–20 | |
| South Pole Observatory | Remote | 1973–2015 | 17–40 | |
| China | Rural | 2014–2017 | 34 | Dufour et al. (2021) |
| Central east China | | | 36 | |
| Beijing–Tianjin–Hebei region | | | 39 | |
| Yangtze River Delta | | | 35 | |
| Pearl River Delta | | | 31 | |
| North America, Europe and East Asia (South Korea and Japan) | 3136 rural sites | 2010–2014 | 0–56 and more | Gaudel et al. (2018) |
| North America, Europe and East Asia | 3348 rural sites and 1453 urban sites | 2010–2014 | 0–100 and more | Fleming et al. (2018) |
| North America, Europe and East Asia | Rural | 1996–2005 | 15–55 | Young et al. (2018) |
| North America, Europe and East Asia | Rural and urban sites | 2010–2014 | 10–60 | Schultz et al. (2017) |
| Eastern North America | Rural<br>Urban | 2000–2014 | 26–38<br>28–38 | Chang et al. (2017) |

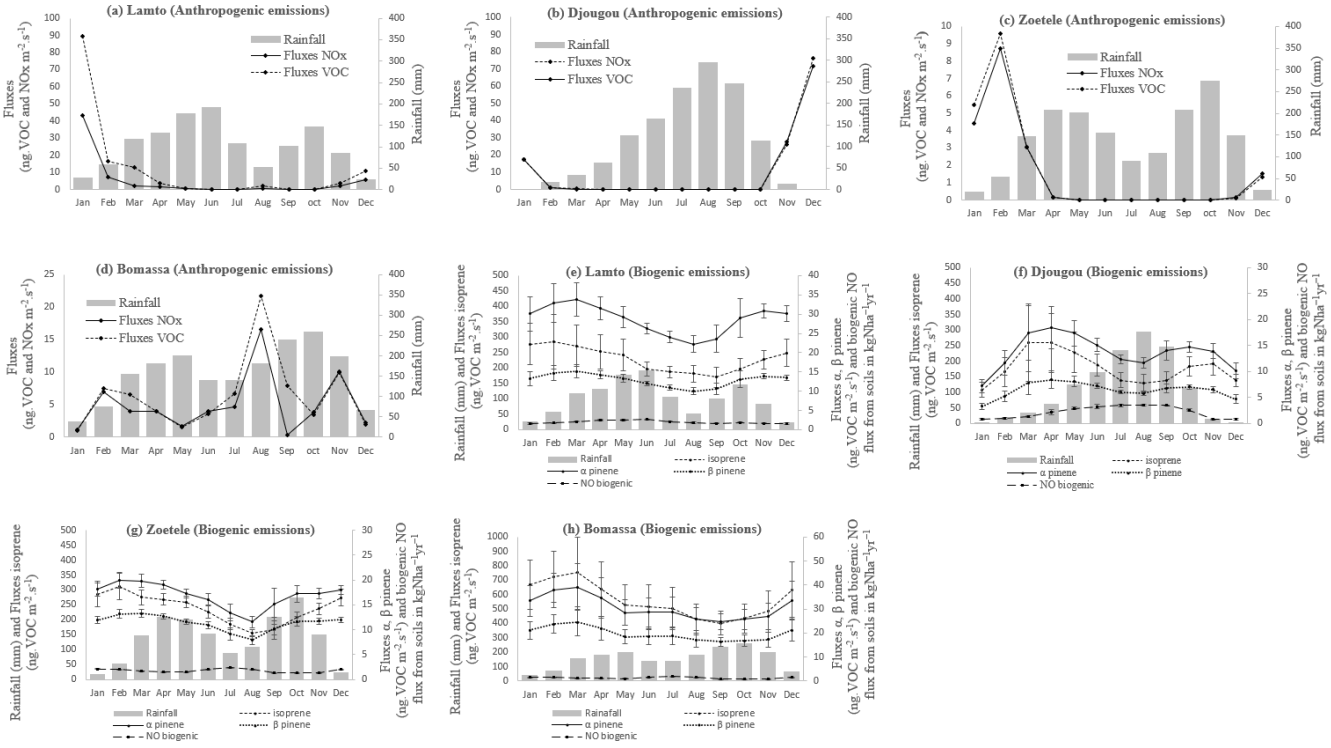


**Figure 8.** Mean monthly fluxes of natural and anthropogenic $NO_x$ and VOC estimated by the GFED4 and MEGAN inventories for $0.25° \times 0.25°$ grid cells centred on each of the wet-savanna and forest sites.

observed at the four sites resembled typical trends for $O_3$ in continental South Africa, with $O_3$ concentrations peaking in late winter and early spring (Laban et al., 2018). The assessment of long-term seasonal and interannual trends of a 21-year ozone passive sampling (monthly means) dataset collected at the Cape Point Global Atmosphere Watch (CPT GAW) station indicated that the annual mean ozone level in this coastal area is 26 ppb (Swartz et al., 2020b), while at Louis Trichardt (1995–2015), Amersfoort (1997–2015) and Skukuza (2000–2015), the level ranged from 22 to 31 ppb (Swartz et al., 2020a). Over the sites of Botswana (1999–2001) and the Mpumalanga Highveld, Zunckel et al. (2004) emphasized that the springtime maximum of $O_3$ concentrations is between 40 and 60 ppb but reached more than 90 ppb as a mean in October 2000. At the background stations at Cape Point (2000–2002), in Namibia (2000–2002) and in areas adjacent to the Highveld, the maximum concentrations are between 20 and 30 ppb with minima between 10 and 20 ppb. Ngoasheng et al. (2021) have investigated the surface ozone concentrations during the periods from 2014 to 2015 and from 2018 to 2019 over 10 sites located in the north-west of South Africa (8–48 ppb). In addition, a more intensive campaign was conducted in June, July and August 2019 during which 15 additional sites were also monitored. During the campaign from September 1999 to June 2001 of the newly established WMO GAW Urban Research Meteorology and Environment (GURME) project, the mean values of ozone concentrations over the sites of Elandsfontein (35.1 ppb) and Cape Point (24.2 ppb) in South Africa, Tamanrasset in Algeria (33.2 ppb), and Mt Kenya (31.5 ppb) indicated high values over many sites (Carmichael et al., 2003). Over a period of 9 to 11 years (1995–2005) at four remote sites – Louis Trichardt (South Africa), Cape Point (South Africa), Amersfoort (South Africa) and Okaukuejo (Namibia) in southern Africa – Martins et al. (2007) demonstrated a fairly constant high mean value of ozone of about 27 ppb throughout the region except for at the Louis Trichardt site, with a relatively high 10-year mean of 35 ppb. These values are approximately 2 times higher compared to western and central Africa INDAAF ozone data. The main reason for this could be the proximity of South Africa sites to $O_3$ precursor sources. They are generally located close to industrial, commercial and residential areas, not far from road traffic, garbage dumps, etc., where precursor emissions are high. Some sites may also be influenced by continental air masses containing gaseous pollutants. From 2012 to 2015, Hamdun and Arakaki (2015) measured surface ozone levels at three urban sites (Mapipa, Ubungo and Posta) and two suburban sites (Kunduchi and Vijibweni) in the city of Dar es Salaam and in the village of Mwetemo, a rural area of Bagamoyo, Tanzania. Ozone levels at suburban sites (7.9–23.6 ppb) were generally higher than at urban sites (10.3–18.6 ppb). In the context of the POLCA programme, $O_3$ was measured using a passive sampling technique from January 2008 to De-

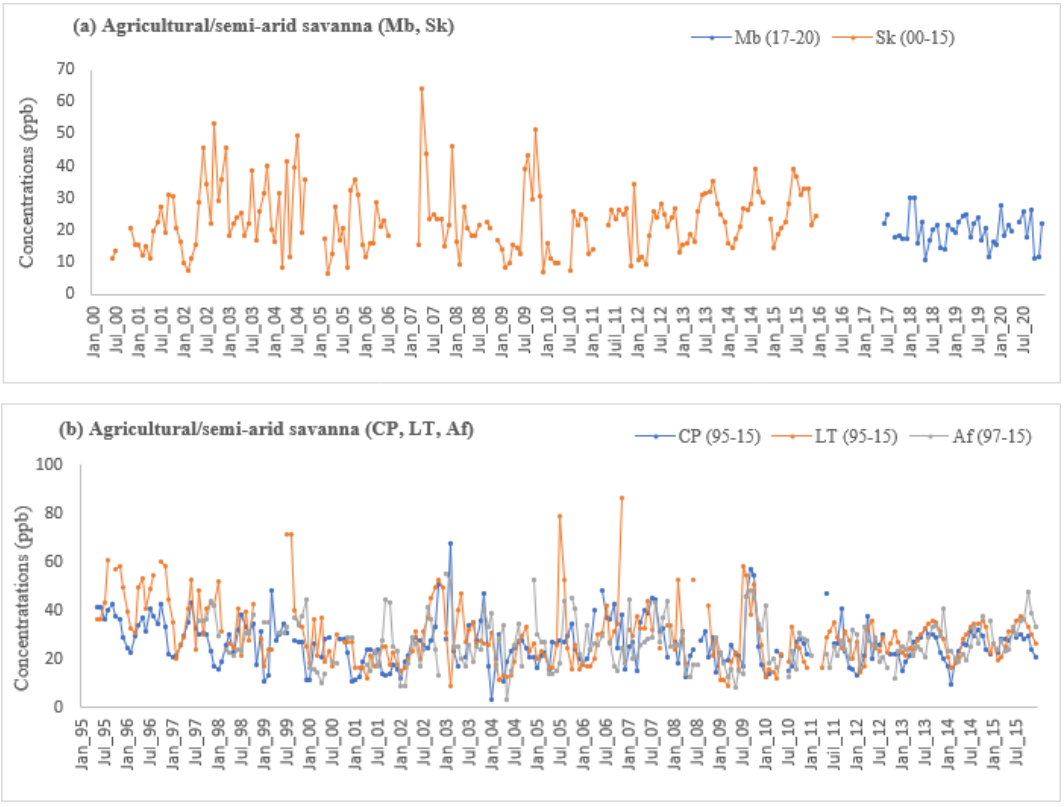


**Figure 9.** Monthly evolution of $O_3$ concentrations (ppb) in agricultural–semi-arid savanna at **(a)** Mb (Kenya) and Sk (South Africa) and **(b)** CP, LT and Af (South Africa).

cember 2009 at Dakar and from June 2008 to December 2009 at Bamako (Adon et al., 2016). The mean annual concentrations of $O_3$ are 7.7 ppb in Dakar and 5.1 ppb in Bamako. At Abidjan during an intensive campaign within the dry season (15 December 2015 to 16 February 2016) and using INDAAF passive samplers exposed in duplicate for 2-week periods (Bahino et al., 2018), the highest $O_3$ concentrations measured were at the two coastal sites of Gonzagueville and Félix Houphouët-Boigny International Airport located in the south-east of the city, with average concentrations of $19.1 \pm 1.7$ and $18.8 \pm 3.0$ ppb, respectively. At urban sites such as Al Ain, Bamako, Dakar, Abidjan and Cotonou, the low $O_3$ levels are due to the saturated $NO_x$ regime observed at these sites, which limits photochemical $O_3$ production (Adon et al., 2013; Bahino et al., 2018; Salem et al., 2009). At most INDAAF sites, concentrations are lower because of the sites' rural characteristics, being generally far from anthropogenic sources and much more influenced by biogenic activities from soils and vegetation. In the framework of the IDAF programme, Adon et al. (2010) analysed ozone concentrations from 2000 to 2007 over the sites of Banizoumbou (Niger), Katibougou and Agoufou (Mali), Djougou (Benin), Lamto (Côte d'Ivoire), Zoétélé (Cameroon), and Bomassa (Congo). Annual mean $O_3$ concentrations are lower for all ecosystems and range from $4.0 \pm 0.4$ ppb (Bomassa) to $14.0 \pm 2.8$ ppb (Djougou) and are of the same order of magnitude over the period of 2000–2020 (INDAAF programme), when concentrations ranged from $3.9 \pm 1.1$ ppb (Bomassa) to $14.8 \pm 4.3$ ppb (Bambey) in western and central Africa. Results are fairly illustrative of the various mitigation or vigilance measures that need to be adopted to ensure the environmental well-being of each ecosystem. Additional efforts must therefore be made through programmes to enhance the density of monitoring networks for polluting gases in general and $O_3$ in particular, especially in Africa, where very few long-term monitoring programmes exist.

### 3.3 Annual and seasonal trends of $O_3$ and its precursors

#### 3.3.1 Annual trends

Annual trends in $O_3$ concentrations were calculated at all sites (except Bambey and Mbita, which do not have 10 years of measurements) according to 95 % confidence intervals in Mann–Kendall tests in dry savanna, wet savanna, forest and agricultural–semi-arid savanna (Fig. 14). At the decade scale, the Katibougou site in Mali shows a decrease in $O_3$ concentrations of around $-2.4$ ppb per decade from 2001 to 2020 ($p$ value $= 0.002$) at the 95 % confidence level (Table 6). This trend at Katibougou is confirmed in both the

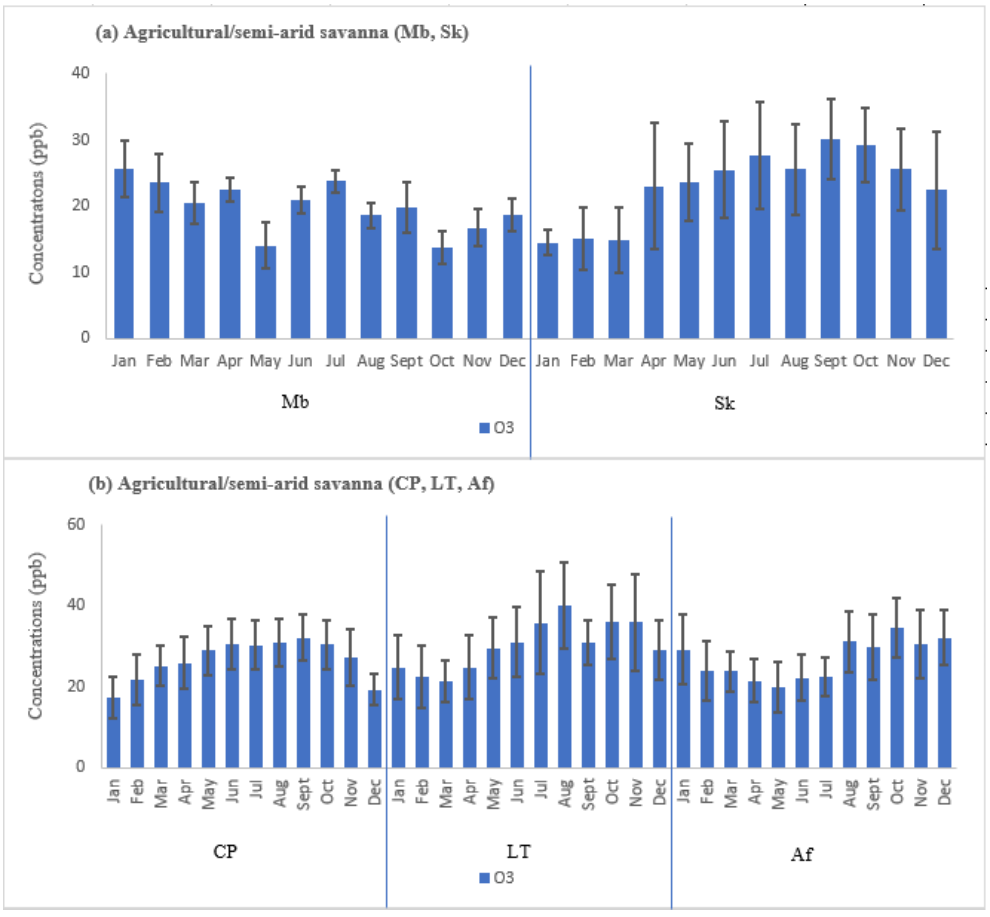


**Figure 10.** Mean monthly averages of $O_3$ concentrations (ppb) in agricultural–semi-arid savanna at **(a)** Mb (Kenya) and Sk (South Africa) and **(b)** CP, LT and Af (South Africa). Mean monthly averages are calculated from the long ozone data series of Fig. 9. Bars represent mean absolute deviation.

dry and the wet seasons. Ozone concentrations decrease by $-1.8$ ppb per decade ($p$ value $= 0.03$) in the dry season and $-3.3$ ppb per decade ($p$ value $< 0.01$) in the wet season. At the same site, the trend in nitrogen oxide ($NO_2$) over the 1998–2020 period shows a decline in annual concentrations and annual seasonal means. Ossohou et al. (2019) observed a decrease in $NO_2$ concentrations at Katibougou in the wet season ($-0.4$ ppb per decade) over the period 1998–2015. These downward trends in $NO_2$ could therefore explain the downward trends in $O_3$. At the Banizoumbou site (Niger), a medium decreasing trend of $-0.8$ ppb per decade in $O_3$ concentrations ($p$ value $= 0.1$) is noted at a 95 % confidence level (Table 6). During the dry period, this downward trend is around $-1.5$ ppb per decade ($p$ value $= 0.04$). The calculation of trends for biogenic VOCs at Banizoumbou indicates a decrease in biogenic emissions of $\alpha$-pinene ($\tau = -0.37$; $p$ value $= 0.020$) and $\beta$-pinene ($\tau = -0.39$; $p$ value $= 0.01$). Chen et al. (2018) indicated that trends in global tree cover from 2000 to 2015 have led to clear decreases, particularly in west Africa, with a reduction of around 10 % in regional BVOC emissions due to agricultural expansion. A weak indication of a downward change in ozone is observed at Agoufou (Mali). At Dahra (Senegal) and in the wet-savanna sites of Lamto (Côte d'Ivoire) and Djougou (Benin), annual ozone trends are not significant (Table 6). In west Africa generally, we note a decrease in surface ozone concentrations even if this trend is not significant at almost all sites. At these remote sites, this decrease could be partly linked to a large decrease in burned area in tropical savannas in Africa, particularly those with low and intermediate levels of tree density (Andela et al., 2017). At the Bomassa site (Congo) ($p$ value $= 1$), we have no trend; this is in contrast to Zoétélé (Cameroon), where a medium increase is recorded in $O_3$ concentrations of 0.5 ppb per decade. To explain the trends observed at Zoétélé, we apply the Kendall rank correlation between $O_3$ concentrations and $O_3$ precursors. We obtain a significant positive rank correlation at the 95 % confidence level. For $NO_x$ and anthropogenic VOCs, $\tau = 0.7$ ($p$ value $= 0.03$), while with biogenic VOCs, the correlation varies from 0.54 to 0.69 ($p$ value $< 0.01$). In addition, we observe increasing trends for biogenic VOCs. Isoprene increases by 18 ng m$^{-2}$ s$^{-1}$ per decade ($p$ value $= 0.001$), $\alpha$-

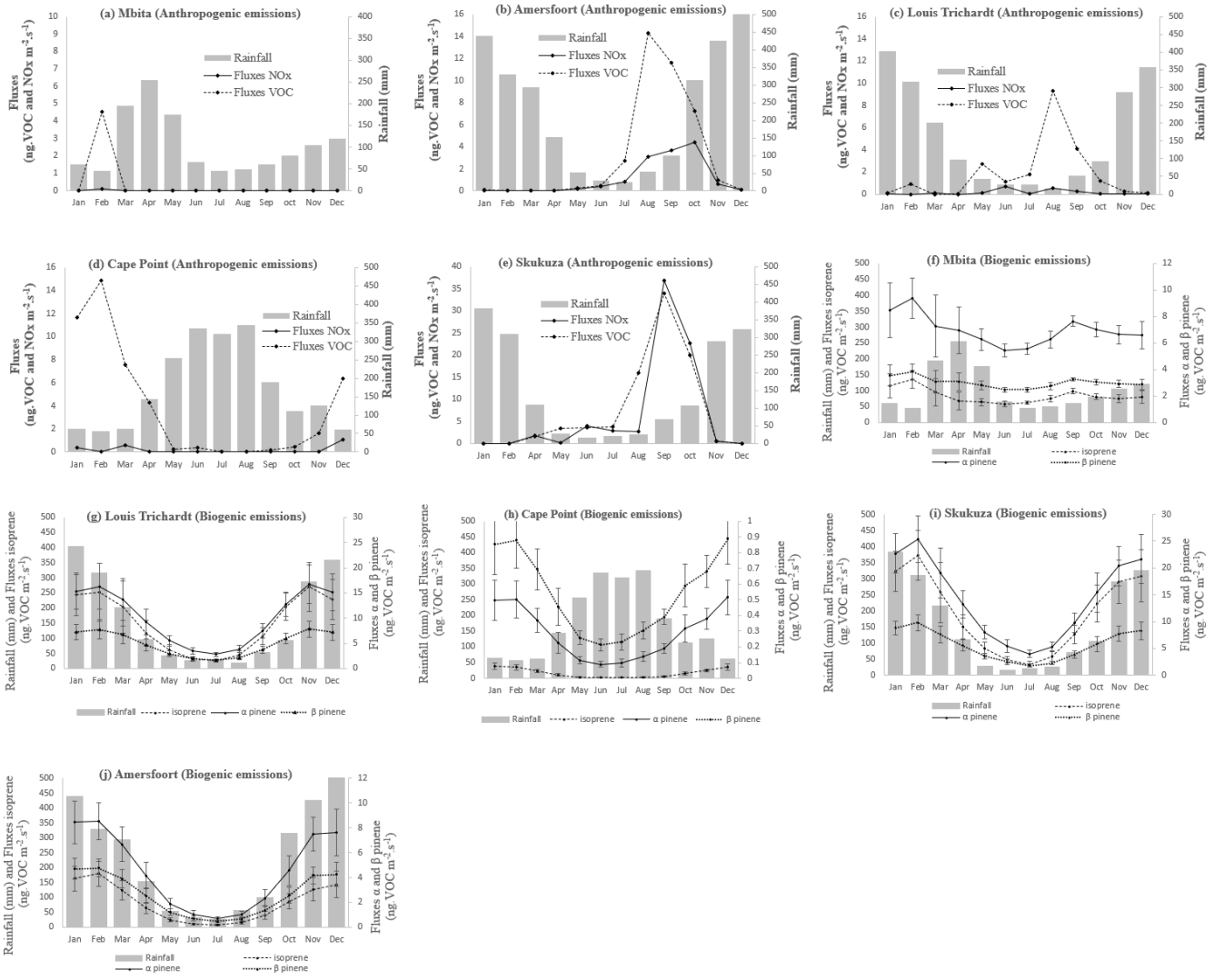


**Figure 11.** Mean monthly fluxes of natural and anthropogenic $NO_x$ and VOC estimated by the GFED4 and MEGAN inventories for $0.25° \times 0.25°$ grid cells centred on each of the agricultural–semi-arid-savanna sites.

pinene by 1 ng $m^{-2}$ $s^{-1}$ per decade ($p$ value $< 0.001$) and $\beta$-pinene by 0.4 ng $m^{-2}$ $s^{-1}$ per decade ($p$ value $= 0.003$). Similar trends were also observed in the wet season for $\alpha$-pinene and $\beta$-pinene and in the dry season for isoprene. The rise in $O_3$ concentrations in Zoétélé could therefore be explained by these increasing trends observed in isoprene, $\alpha$-pinene and $\beta$-pinene from one season to the other and in anthropogenic emissions in African forest regions. These results are corroborated by 18 years of satellite data (1998–2015) in Andela et al. (2017), who noted an increasing trend in the burned areas of closed-canopy forests. In South African sites, at Louis Trichardt ($p$ value $= 0.48$), Amersfoort ($p$ value $= 0.44$) and Skukuza, no trend is reported; this is in contrast to Cape Point, where we observe a weak downward trend of ozone (Table 6) at a confidence level of 95 %.

**Table 6.** Annual tend of ozone concentrations over the period 1995–2020 for 12 measurement sites.

| Station name | Trend (ppb per decade) | $p$ value | Analysis of annual trend values |
|---|---|---|---|
| Banizoumbou | $-0.8 \pm 0.7$ | 0.1 | Medium downward trend |
| Katibougou | $-2.4 \pm 0.5$ | 0.002 | Downward trend |
| Agoufou | $-1.9 \pm 0.1$ | 0.21 | Weak downward trend |
| Dahra | $-2.6 \pm 2.7$ | 0.35 | No trend |
| Lamto | $-0.3 \pm 0.2$ | 0.6 | No trend |
| Djougou | $-0.3 \pm 0.3$ | 0.55 | No trend |
| Zoétélé | $0.5 \pm 0.2$ | 0.09 | Medium upward trend |
| Bomassa | $-0.003 \pm 0.3$ | 1 | No trend |
| Louis Trichardt | $-3.4 \pm 2.0$ | 0.48 | No trend |
| Skukuza | $2.2 \pm 0.4$ | 0.5 | No trend |
| Amersfoort | $-1.1 \pm 0.5$ | 0.44 | No trend |
| Cape Point | $-2.7 \pm 0.3$ | 0.14 | Weak downward trend |

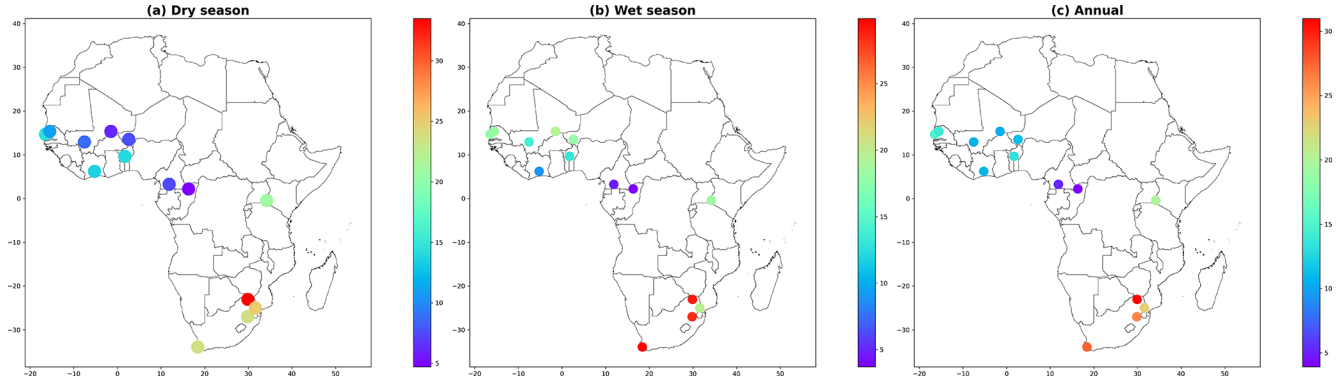


**Figure 12.** Seasonal and annual mapping of $O_3$ concentration levels **(a)** in the dry season (Ba, Ka, Ag, Da and Bb: October to May; La and Dj: November to March; Zo: December to February and July to August; Bo: December to February; Mb: June to October and January to February; LT, Sk and Af: April to September; CP: October to March), **(b)** in the wet season (Ba, Ka, Ag, Da and Bb: June to September; La and Dj: April to October; Zo: March to June and September to November; Bo: March to November; Mb: March to May and November to December; LT, Sk and Af: October to March; CP: April to September) and **(c)** annually over the 14 studied sites. Publisher's remark: please note that the above figure contains disputed territories.

The absence of annual trends at South African sites assessed with certainty confirms the results obtained by Swartz et al. (2020a, b) at the Louis Trichardt, Amersfoort, Skukuza and Cape Point sites using multiple-linear-regression model approach. Indeed, the trend lines for the $O_3$ concentrations measured during the whole of each sampling period indicate slight negative slopes at Amersfoort and Louis Trichardt and a small positive slope at Skukuza (Swartz et al., 2020a). Gaudel et al. (2020, 2024) have observed that annual trends of median ozone values have increased in the tropospheric column (IAGOS, 950 to 200 hPa) by around 2 nmol mol$^{-1}$ per decade during 22 years (1994–2016) of measurements and by $2.43 \pm 0.48$ nmol mol$^{-1}$ per decade (1994–2019) above the Gulf of Guinea. Trends are confirmed by new OMI/MLS satellite data covering the period 2004–2019 at the same sites, with tropical tropospheric ozone trends indicating values of around $0.41 \pm 0.80$ nmol mol$^{-1}$ per decade (Gaudel et al., 2024). These results are contrary to the decrease in ozone observed at the INDAAF sites in the Gulf of Guinea (Lamto and Djougou), which show no trend. To partly explain the increase in ozone in recent decades, Gaudel et al. (2020) pointed out that although $NO_x$ emissions from biomass combustion have decreased in the tropics, this decrease has been overcompensated by the increase in fossil fuel emissions. However, we believe that the discrepancy between these studies could be explained by the proximity of the measurement sites to the sources of precursor emissions. Indeed, the data measured from the commercial aircraft monitoring network used in the work of Gaudel et al. (2020, 2024) are taken at airports closer to cities, whereas INDAAF sites are rural sites far from fossil fuel combustion sources. In addition, Gaudel et al. (2018) reported that spatially, global surface ozone trends are highly variable depending on the time period, region, elevation and proximity to fresh ozone precursor emissions. The distributions of ozone annual trends in the most recent 2 decades (2000–2019) explored by Hou et al. (2023) over six regions of the world including Africa (25° S–25° N, 17° W–51° E) showed a significant increase in the tropospheric column ozone in these six regions (OMI/MLS satellite data), with the smallest value of $\sim 0.07$ DU yr$^{-1}$ in Africa, while with the MET+2015EMIS model, the annual trends of ozone over Africa show insignificant decreases (0.04 DU yr$^{-1}$). These trends, which are relatively small and which contrast with the changes observed at most INDAAF sites, could support the claim that ozone surface data do not necessarily represent the free troposphere, where the radiative forcing effects of ozone are concentrated. We also think that for ozone trends to be estimated more accurately, it is necessary to combine soundings and long-term surface observations. Breaks in the annual concentration data were observed, as a result of the Pettitt test, at Banizoumbou and Katibougou in 2006. During the dry and wet seasons, further breaks were recorded in the annual series in 2006 (Katibougou) and 2007 (Banizoumbou) (dry season) and in 2014 at Katibougou (wet season). However, no trend inversion was induced in these break years. At the other study sites, no breaks were observed.

### 3.3.2 Seasonal trends

Trend tests were performed on monthly mean $O_3$ concentrations using seasonal Kendall tests and all trend results are presented in Fig. 15. The tests reveal a significant downward trend of $-0.7$ ppb per decade at Banizoumbou ($p$ value $= 0.02$) at the 95 % confidence level. At Katibougou ($p$ value $< 0.001$), $O_3$ concentrations decrease by $-2.4$ ppb per decade. At the other sites in west Africa, downward trends in $O_3$ of $-0.7$ ppb per decade at Agoufou, $-0.6$ ppb per decade at Dahra and $-0.23$ ppb per decade at Lamto are calculated. However, the significance is medium

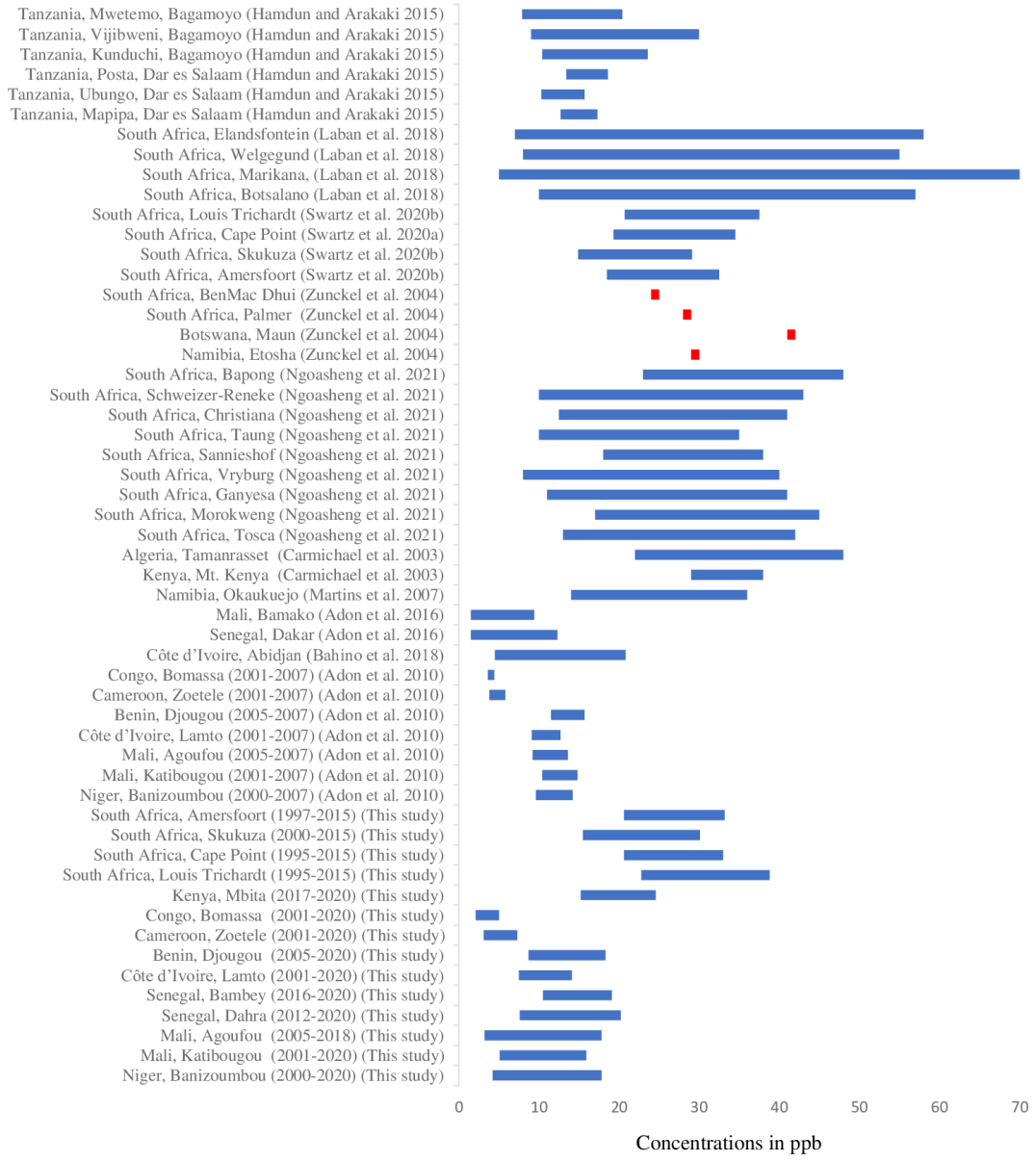


**Figure 13.** Overview of $O_3$ monitoring studies in Africa. Blue bars represent lower and upper ranges of means if reported. Red points represent average concentrations of $O_3$.

at Agoufou and low at Dahra and Lamto at the 95 % confidence interval. There is no trend at Djougou. The trends in Bomassa ($p$ value = 0.17) and Cape Point ($p$ value = 0.13) are similar to those at sites of west Africa. At the Louis Trichardt and Amersfoort sites, the results show no ozone trend ($p$ value = 0.67 and 0.93) but −2.7 and −0.1 ppb per decade decreases, respectively. In contrast, an upward trend is reported at Zoétélé in Cameroon (Sen slope = +0.7 ppb per decade; $p$ value = 0.001) and at Skukuza in South Africa (Sen slope = +3.4 ppb per decade; $p$ value = 0.001) at the 95 % confidence interval. All the annual trends observed at INDAAF sites are confirmed by Kendall's seasonal trends.

The $O_3$ mixing ratio in the lower troposphere is slightly higher in central Africa in July than in northern Africa (in January), likely indicating rapid photochemical $O_3$ production by biomass burning precursors (Singh et al., 1996) during the Southern Hemisphere fires (Tsivlidou et al., 2023). Biomass burning air mass transport from the hemisphere where fires occur (where the highest CO is measured) to the opposite hemisphere is enabled by either the north-easterly harmattan flow (January) or the south-easterly winds and monsoon flow (July) (Sauvage et al., 2005; Tsivlidou et al., 2023) and could also explain the upward trend observed at Zoétélé. At Skukuza, the upward trend is thought

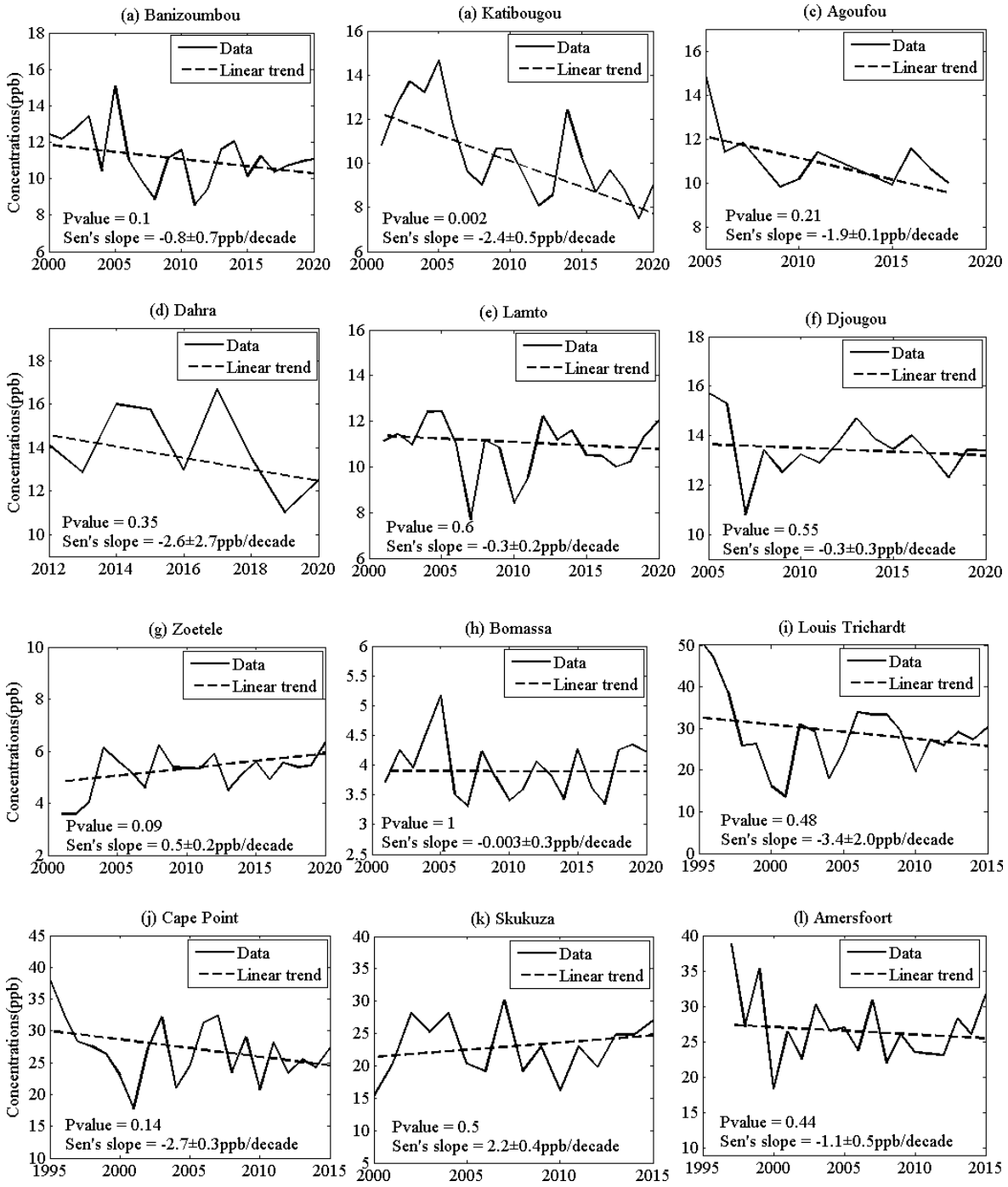


**Figure 14.** Long-term annual linear trend of in situ $O_3$ concentrations over the period 1995–2020 at 95 % confidence intervals, calculated for 12 measurement sites representative of African dry savanna, wet savanna, forest and agricultural–semi-arid savanna and the *p* value for each trend.

to be due to anthropogenic emissions. At the Irene site in the north-eastern interior of South Africa, Bencherif et al. (2020) obtained an upward trend in the tropospheric $O_3$ column (1998–2017) at a rate of around 2.4 % per decade. At Irene, an increase in tropospheric ozone is reported by Thompson et al. (2014) from September to November and by Mulumba et al. (2015) from December to February from ozonesonde records (1990–2008) and ozone tropospheric columns (1998–2013). An upward trend in $NO_2$ levels was also evident at Skukuza, signifying the influence of growing rural communities on the Kruger National Park border (Swartz et al., 2020a). At the South African sites, high

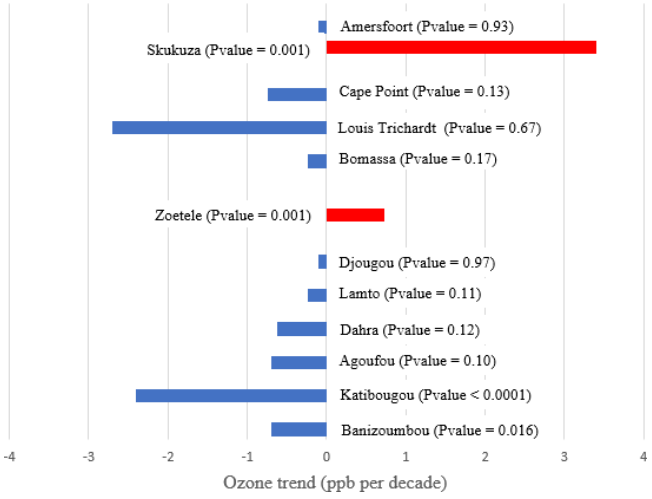


**Figure 15.** Kendall's seasonal trend of in situ $O_3$ concentrations over the period 1995–2020 at 95 % confidence intervals calculated for 12 measurement sites representative of African dry savanna, wet savanna, forest and agricultural–semi-arid savanna and the $p$ value for each trend.

values of $NO_x$ and VOC fluxes are observed at Skukuza (Fig. 11d). Population growth and the associated increase in anthropogenic activities (like domestic biomass burning and solid fuel combustion) result in high levels of pollutants in South Africa's Highveld region (Kai et al., 2022; Keita et al., 2021) and could therefore explain the upward trend obtained. The increase in $O_3$ in South Africa could also be explained by biomass burning (agricultural reason) and greenhouse (urban-industry reason) activities implemented in Africa during the summer and spring seasons (Bencherif et al., 2020; Diab et al., 2004; Sivakumar and Ogunniyi, 2017). Furthermore, pollutant emissions from domestic biofuel, brought by long-range transport of pollution in the Southern Hemisphere, have an impact at the continental scale (Thompson et al., 2014). Moreover, Thompson et al. (2021) have observed an increasing mean trend of +1.2 % per decade ($p$ value = 0.119) from 22-year SHADOZ records (1998–2019) of ozone profiles in the free troposphere (5–15 km) in Nairobi in east Africa. This trend result is similar to surface ozone change observed in Skukuza. The increase in tropospheric ozone in the tropics, partly of dynamic origin due to the movement of air masses and not solely due to growing anthropogenic emissions (Thompson et al., 2021), could also explain this similarity. Balashov et al. (2014) reported that the sites of Palmer and Makalu over the South African Highveld exhibited statistically significant negative trends in surface ozone from 1990 to 2007 over the spring season and the month of September, whereas Verkykkop and Elandsfontein showed no statistically significant change in surface ozone. At most INDAAF sites (remote and rural) we found, as in the work of Balashov et al. (2014), that the surface ozone data showed no trend. These results confirm, however, that surface ozone trends in Africa are not regionally or seasonally uniform, as mentioned by Thompson et al. (2021).

## 4 Conclusion

This work presents an original database of long-term $O_3$ concentrations at 14 African sites belonging to the INDAAF programme and companion projects. This database gives a better understanding of $O_3$ concentration levels at remote tropical sites representative of the major African biomes. In this study, we establish a mean annual cycle by site and ecosystem type and investigate the seasonal variability in $O_3$ concentrations over the period 1995–2020. Our analysis of the seasonality of anthropogenic and biogenic $NO_x$ and VOC emissions then highlights the significant factors contributing to $O_3$ formation. Finally, we calculate the $O_3$ long-term trends, which provide an insight into the long-term evolution of $O_3$ levels and the local and regional dynamics of the emission sources of $O_3$ precursors.

The results indicated that $O_3$ levels are the highest during the rainy season in dry savannas and during the dry season in wet savannas and forests. In agricultural fields, no seasonal variations in $O_3$ concentrations are observed. In the semi-arid savanna (South Africa), dry-season $O_3$ levels are the highest at Louis Trichardt and Skukuza. At the Cape Point and Amersfoort sites, maxima occur during the rainy season. Mean annual $O_3$ concentrations range from $10.5 \pm 5.4$ to $14.8 \pm 4.3$ ppb in dry savannas, from $10.8 \pm 3.3$ to $13.5 \pm 4.8$ ppb in wet savannas, from $3.9 \pm 1.1$ to $5.2 \pm 2.1$ ppb in forest ecosystems and from $19.9 \pm 4.7$ to $30.8 \pm 8.0$ ppb in agricultural–semi-arid savannas. BVOCs (under the influence of air temperature), NO emissions (in the presence of humidity) and precipitation are the main contributors to $O_3$ formation in dry savannas. The seasonality of $O_3$ measurements and dominant precursors confirms the important role of microbial processes that lead to high NO emissions at the beginning of the wet season in $O_3$ production. Furthermore, the influence of air temperature and solar radiation on woody emissions from shrubs in the Sahel and the presence of sparse vegetation (short grasses, forbs and dicotyledonous shrubs with perennial ground cover) in this region could be at the origin of BVOC emissions. The photochemical $O_3$ regime in savannas and rainforests (heavily vegetated areas) is strongly linked to BVOC emissions from vegetation and to temperature, radiation and humidity. At Lamto and Zoétélé, anthropogenic $NO_x$ and VOC also contribute to $O_3$ formation. The most dominant precursors in southern Africa are mainly $NO_x$ emissions (anthropogenic and biogenic), humidity and temperature, as well as anthropogenic VOCs at a few sites. They occur due to biomass and fuel combustion, large-scale transport of pollutants, domestic combustion in winter, and biogenic emissions from vegetation. At INDAAF sites, which are rural sites far from many anthropogenic sources, $O_3$ concentrations are below

most of the values reported in the literature. At 95 % confidence intervals, annual and seasonal trends (based on Mann–Kendall treatment and low $p$ values) indicate that the Katibougou site in Mali and the Banizoumbou site in Niger experience a significant decrease in $O_3$ concentrations, around $-2.4$ and $-0.8$ ppb per decade, respectively, with a high certainty over the period 2000 to 2020. These likely result from downward trends in $NO_2$ observed at Katibougou and reduced BVOC emissions at Banizoumbou. In contrast, a significant upward trend is reported at Zoétélé ($+0.7$ ppb per decade) in Cameroon and Skukuza ($+3.4$ ppb per decade) in South Africa. These trends are attributed to the increase in BVOCs in Zoétélé and increases in anthropogenic emissions that affect Skukuza.

This study described the $O_3$ levels, as well as photochemical and meteorological regimes related to seasonal concentrations and their derived trends, in representative African biomes. The results on regional trend variability and seasonal variations are consistent with published studies of African ozone data, although in most cases, the INDAAF measurements are more rural than data taken at urban monitoring sites, including airports. The importance of developing, and maintaining long-term observations like those of the INDAAF project, with regular calibration and standards, cannot be overstated. In particular, for the INDAAF is mostly agricultural locations, the data can be used to assess the impact of $O_3$ dry-deposition fluxes on African crops and the potential crop yield losses because of $O_3$ toxicity to plants. Studies of ozone changes during the growing season can lead to action plans for achieving better food security. The ozone data provide invaluable constraints for models of chemical and climate processes in the atmosphere. With INDAAF data and improved models, there will be more confidence in future predictions of African air quality and of the exposure of agriculture and the regional population to surface ozone.

**Data availability.** Dataset DOIs of $O_3$ observations for INDAAF sites, available via the INDAAF database at https://indaaf.obs-mip.fr, are as follows:

- Banizoumbou (Niger) – https://doi.org/10.25326/608 (Laouali et al., 2023)
- Katibougou (Mali) – https://doi.org/10.25326/604 (Galy-Lacaux et al., 2023a)
- Agoufou (Mali) – https://doi.org/10.25326/610 (Galy-Lacaux et al., 2023b)
- Bambey (Senegal) – https://doi.org/10.25326/609 (Galy-Lacaux et al., 2023c)
- Dahra (Senegal) – https://doi.org/10.25326/606 (Galy-Lacaux et al., 2023d)
- Lamto (Côte d'Ivoire) – https://doi.org/10.25326/275 (Galy-Lacaux et al., 2023e)
- Djougou (Benin) – https://doi.org/10.25326/605 (Akpo et al., 2023)
- Zoétélé (Cameroon) – https://doi.org/10.25326/603 (Ouafo-Leumbe et al., 2023)
- Bomassa (Congo) – https://doi.org/10.25326/607 (Galy-Lacaux et al., 2023f)
- Mbita (Kenya) – https://doi.org/10.25326/642 (Galy-Lacaux et al., 2023g)
- Louis Trichardt (South Africa) – https://doi.org/10.25326/646 (van Zyl et al., 2023a)
- Skukuza (South Africa) – https://doi.org/10.25326/645 (van Zyl et al., 2023b)
- Cape Point (South Africa) – https://doi.org/10.25326/644 (van Zyl et al., 2023c)
- Amersfoort (South Africa) – https://doi.org/10.25326/647 (van Zyl et al., 2023d).

GFED4 ($NO_x$, VOCs) and MEGAN-MACC (isoprene, $\alpha$-pinene, $\beta$-pinene) data are available at https://eccad.sedoo.fr/#/data (login required; Zilbermann et al., 2024). ERA5 reanalysis data are available at https://climate.copernicus.eu/climate-reanalysis (ECMWF, 2023).

**Author contributions.** CGL designed the study, wrote the protocol and edited the paper. HEVD conducted data processing and the statistical analysis and wrote the paper. CD made conceptual contributions and edited the paper. ABA and MO contributed to the statistical analysis, assisted in sample collection and edited the paper. VY, DL, MOL, ON and PGVZ assisted in sample collection and edited the paper. EG and MDA analysed the samples.

**Competing interests.** The contact author has declared that none of the authors has any competing interests.

**Disclaimer.** Publisher's note: Copernicus Publications remains neutral with regard to jurisdictional claims made in the text, published maps, institutional affiliations, or any other geographical representation in this paper. While Copernicus Publications makes every effort to include appropriate place names, the final responsibility lies with the authors.

**Special issue statement.** This article is part of the special issue "Tropospheric Ozone Assessment Report Phase II (TOAR-II) Community Special Issue (ACP/AMT/BG/GMD inter-journal SI)". It is not associated with a conference.

**Acknowledgements.** The authors would like to acknowledge the INDAAF project (International Network to study Deposition and Atmospheric chemistry in AFrica) and especially all its local technicians for their maintenance and sampling work. We would also like to acknowledge the Cycle de l'Azote entre la Surface et l'Atmosphère en afriQUE (CASAQUE) project and the International Nitrogen Management System (INMS) for providing us with data on $O_3$ concentrations at Dahra and Mbita. This study was supported by the INSA (Integrated Nitrogen Studies in Africa) project,

which funded the research carried out for this paper at the Laboratoire d'Aérologie in Toulouse. We are indebted to the AMMA-CATCH project, the University of Copenhagen and the Observatoire de recherche en environnement "Bassins versants tropicaux expérimentaux" (SO BVET) for providing us with meteorological data from Niger, Benin, Senegal and Cameroon. We are also grateful to the ECCAD platform and the European Centre for Medium-Range Weather Forecasts (ECMWF) for biogenic and anthropogenic emissions and ERA5 reanalysis data.

**Financial support.** This research has been supported by the European Union's EU Horizon 2020 research and innovation programme under the Marie Skłodowska-Curie Actions (grant no. 871944).

**Review statement.** This paper was edited by Yugo Kanaya and reviewed by three anonymous referees.

## References

Abbadie, L. (Ed.): Lamto: Structure, Functioning, and Dynamics of a Savanna Ecosystem, Ecological Studies, Springer Science+Business Media, New York, 415 pp., ISBN 9780387948447, 2006.

Abiodun, B. J., Ojumu, A. M., Jenner, S., and Ojumu, T. V.: The transport of atmospheric $NO_x$ and $HNO_3$ over Cape Town, Atmos. Chem. Phys., 14, 559–575, https://doi.org/10.5194/acp-14-559-2014, 2014.

Adon, M., Galy-Lacaux, C., Yoboué, V., Delon, C., Lacaux, J. P., Castera, P., Gardrat, E., Pienaar, J., Al Ourabi, H., Laouali, D., Diop, B., Sigha-Nkamdjou, L., Akpo, A., Tathy, J. P., Lavenu, F., and Mougin, E.: Long term measurements of sulfur dioxide, nitrogen dioxide, ammonia, nitric acid and ozone in Africa using passive samplers, Atmos. Chem. Phys., 10, 7467–7487, https://doi.org/10.5194/acp-10-7467-2010, 2010.

Adon, M., Galy-Lacaux, C., Delon, C., Yoboue, V., Solmon, F., and Kaptue Tchuente, A. T.: Dry deposition of nitrogen compounds ($NO_2$, $HNO_3$, $NH_3$), sulfur dioxide and ozone in west and central African ecosystems using the inferential method, Atmos. Chem. Phys., 13, 11351–11374, https://doi.org/10.5194/acp-13-11351-2013, 2013.

Adon, M., Yoboue, V., Galy-Lacaux, C., Liousse, C., Diop, B., Doumbia, E. H. T., Gardrat, E., Ndiaye, S. A., and Jarnot, C.: Measurements of $NO_2$, $SO_2$, $NH_3$, $HNO_3$ and $O_3$ in West African urban environments, Atmos. Environ., 135, 31–40, https://doi.org/10.1016/j.atmosenv.2016.03.050, 2016.

Aghedo, A. M., Schultz, M. G., and Rast, S.: The influence of African air pollution on regional and global tropospheric ozone, Atmos. Chem. Phys., 7, 1193–1212, https://doi.org/10.5194/acp-7-1193-2007, 2007.

Akpo, A., Galy-Lacaux, C., Delon, C., Gardrat, E., Dias Alves, M., Lenoir, O., Halisson, J., Darakpa, C., and Darakpa, D.: Trace gases, Djougou, Benin, Aeris [data set], https://doi.org/10.25326/605, 2023.

Andela, N., Morton, C., Giglio, L., Chen, Y., van Der Werf, G., Kasibhatla, P. S., DeFries, R. S., Collatz, G. J., Hantson, S., Kloster, S., Bachelet, D., Forrest, M., Lasslop, G., Li, F., Mangeon, S., Melton, J. R., Yue, C., and Randerson, J. T.: A human-driven decline in global burned area, Science, 356, 1356–1362, https://doi.org/10.1126/science.aal4108, 2017.

Bahino, J., Yoboué, V., Galy-Lacaux, C., Adon, M., Akpo, A., Keita, S., Liousse, C., Gardrat, E., Chiron, C., Ossohou, M., Gnamien, S., and Djossou, J.: A pilot study of gaseous pollutants' measurement ($NO_2$, $SO_2$, $NH_3$, $HNO_3$ and $O_3$) in Abidjan, Côte d'Ivoire: contribution to an overview of gaseous pollution in African cities, Atmos. Chem. Phys., 18, 5173–5198, https://doi.org/10.5194/acp-18-5173-2018, 2018.

Balashov, N. V., Thompson, A. M., Piketh, S. J., and Langerman, K. E.: Surface ozone variability and trends over the South African Highveld from 1990 to 2007, J. Geophys. Res.-Atmos., 119, 4323–4342, https://doi.org/10.1002/2013JD020555, 2014.

Baldy, S., Ancellet, G., Bessafi, M., Badr, A., and Luk, D. L. S.: Field observations of the vertical distribution of tropospheric ozone at the island of Reunion (southern tropics), J. Geophys. Res.-Atmos., 101, 23835–23849, https://doi.org/10.1029/95jd02929, 1996.

Bakayoko, A., Galy-Lacaux, C. Véronique Yoboué, V., Hickman, J., E., Roux, F., Gardrat, E., Julien, F., and Delon, C.: Dominant contribution of nitrogen compounds in precipitation chemistry in the Lake Victoria catchment (East Africa), Environ. Res. Lett, 16, 1–20, https://doi.org/10.1088/1748-9326/abe25c, 2021.

Bencherif, H., Toihir, A. M., Mbatha, N., Sivakumar V., Preez, D. J., Bègue, N., and Coetzee, G.: Ozone Variability and Trend Estimates from 20-Years of Ground-Based and Satellite Observations at Irene Station, South Africa, Atmosphere, 11, 1216, https://doi.org/10.3390/atmos11111216, 2020.

Bigaignon, L., Delon, C., Ndiaye, O. Galy-Lacaux, C., Serça, D., Guérin, F., Tallec, T., Merbold, L., Tagesson, T., Fensholt, R., André, S., and Sylvain Galliau, S.: Understanding $N_2O$ Emissions in African Ecosystems: Assessments from a Semi-Arid Savanna Grassland in Senegal and Sub-Tropical Agricultural Fields in Kenya, Sustainability, 12, 1–26, https://doi.org/10.3390/su12218875, 2020.

Brown, F., Folberth, G. A., Sitch, S., Bauer, S., Bauters, M., Boeckx, P., Cheesman, A. W., Deushi, M., Dos Santos Vieira, I., Galy-Lacaux, C., Haywood, J., Keeble, J., Mercado, L. M., O'Connor, F. M., Oshima, N., Tsigaridis, K., and Verbeeck, H.: The ozone–climate penalty over South America and Africa by 2100, Atmos. Chem. Phys., 22, 12331–12352, https://doi.org/10.5194/acp-22-12331-2022, 2022.

Camredon, M. and Aumont, B.: I-L'ozone troposphérique : production/consommation et régimes chimiques, Pollut. Atmos., 193, 51–60, https://doi.org/10.4267/pollution-atmospherique.1404, 2007.

Carmichael, G. R., Ferm, M., Thongboonchoo, N., Woo, J.-H., Chan, L., Murano, K., Viet, P. H., Mossberg, C., Bala, R., Boonjawat, J., Upatum, P., Mohan, M., Adhikary, S. P., Shrestha, A. B., Pienaar, J., Brunke, E. B., Chen, T., Jie, T., Guoan, D., Peng, L. C., Dhiharto, S., Harjanto, H., Jose, A. M., Kimani, W., Kirouane, A., Lacaux, J.-P., Richard, S., Barturen, O., Cerda, J. C., Athayde, A., Tavares, T., Cotrina, J. S., and Bilici, E.: Measurements of sulfur dioxide, ozone and ammonia concentrations in Asia, Africa, and South America using passive samplers, Atmos. Environ., 37, 1293–1308, https://doi.org/10.1016/S1352-2310(02)01009-9, 2003.

Chang, K.-L., Petropavlovskikh, I., Cooper, I. O. R., Schultz, M. G., and Wang, T.: Regional trend analysis of surface ozone observations from monitoring networks in eastern North America, Europe and East Asia, Elem. Sci. Anth., 50, 1–22, https://doi.org/10.1525/elementa.243, 2017.

Chen, W. H., Guenther, A. B., Wang, X. M., Chen, Y. H., Gu, D. S., Chang, M., Zhou, S. Z., Wu, L. L., and Zhang, Y. Q.: Regional to global biogenic isoprene emission responses to changes in vegetation from 2000 to 2015, J. Geophys. Res.-Atmos., 123, 3757–3771, https://doi.org/10.1002/2017JD027934, 2018.

Clain, G., Baray, J. L., Delmas, R., Diab, R., Leclair de Bellevue, J., Keckhut, P., Posny, F., Metzger, J. M., and Cammas, J. P.: Tropospheric ozone climatology at two Southern Hemisphere tropical/-subtropical sites, (Reunion Island and Irene, South Africa) from ozonesondes, LIDAR, and in situ aircraft measurements, Atmos. Chem. Phys., 9, 1723–1734, https://doi.org/10.5194/acp-9-1723-2009, 2009.

Conradie, E. H., Van Zyl, P. G., Pienaar, J. J., Beukes, J. P., Galy-Lacaux, C., Venter, A. D., and Mkhatshwa, G. V.: The chemical composition and fluxes of atmospheric wet deposition at four sites in South Africa, Atmos. Environ., 146, 113–131, https://doi.org/10.1016/j.atmosenv.2016.07.033, 2016.

Cooper, O. R., Parrish, D. D., Ziemke, J., Balashov, N. V., Cupeiro, M., Galbally, I. E., Gilge, S., Horowitz, L., Jensen, N. R., Lamarque, J.-F., Naik, V., Oltmans, S. J., Schwab, J., Shindell, D. T., Thompson, A. M., Thouret, V., Wang, Y., and Zbinden, R. M.: Global distribution and trends of tropospheric ozone: An observation-based review, Elementa, 2, 1–28, https://doi.org/10.12952/journal.elementa.000029, 2014.

Cooper, O. R., Schultz, M. G., Schröder, S., Chang, K.-L., Gaudel, A., Benítez, G. C., Cuevas, E., Fröhlich, M., Galbally, I. E., Molloy, S., Kubistin, D. Lu, X., McClure-Begley, A., Nédélec, P., O'Brien, J., Oltmans, S. J., Petropavlovskikh, I., Ries, L., Senik, I. Sjöberg, K., Solberg, S., Spain, G. T., Spang, W., Steinbacher, M., Tarasick, D., Thouret V., and Xu, X.: Multi-decadal surface ozone trends at globally distributed remote locations, Elem. Sci. Anth., 8, 1–34, https://doi.org/10.1525/elementa.420, 2020.

Cros, B., Fontan, J., Minga, A., Helas, G., Nganga, D., Delmas, R., Chapuis, A., Benech, B., Druilhet, A., and Andreae, M. O.: Vertical profiles of ozones between 0 and 400 meters in and above the African equatorial Forest, J. Geophys. Res., 97, 12877–12887, 1992.

Darras, S., Granier, C., Liousse, C., Doumbia, T., Keita, S., Soulie, A.: The ECCAD database: Access to a variety of inventories of emissions for greenhouse gases and air pollutants, 35ème colloque annuel de l'Association Internationale de Climatologie – AIC, France, 6–9 July 2022, Toulouse, France, 1–6, http://www.meteo.fr/cic/meetings/2022/aic/ (last access: 26 November 2024), 2022.

Debaje, S. B., Jeyakumar, S. J., Ganesan, K., Jadhav, D. B., and Seetaramayya, P.: Surface ozone measurements at tropical rural coastal station Tranquebar, India, Atmos. Environ., 37, 4911–4916, https://doi.org/10.1016/j.atmosenv.2003.08.005, 2003.

Delon, C., Galy-Lacaux, C., Boone, A., Liousse, C., Serça, D., Adon, M., Diop, B., Akpo, A., Lavenu, F., Mougin, E., and Timouk, F.: Atmospheric nitrogen budget in Sahelian dry savannas, Atmos. Chem. Phys., 10, 2691–2708, https://doi.org/10.5194/acp-10-2691-2010, 2010.

Delon, C., Galy-Lacaux, C., Adon, M., Liousse, C., Serça, D., Diop, B., and Akpo, A.: Nitrogen compounds emission and deposition in West African ecosystems: comparison between wet and dry savanna, Biogeosciences, 9, 385–402, https://doi.org/10.5194/bg-9-385-2012, 2012.

Delon, C., Mougin, E., Serça, D., Grippa, M., Hiernaux, P., Diawara, M., Galy-Lacaux, C., and Kergoat, L.: Modelling the effect of soil moisture and organic matter degradation on biogenic NO emissions from soils in Sahel rangeland (Mali), Biogeosciences, 12, 3253–3272, https://doi.org/10.5194/bg-12-3253-2015, 2015.

Diab, R. D., Raghunandan, A., Thompson, A. M., and Thouret, V.: Classification of tropospheric ozone profiles over Johannesburg based on mozaic aircraft data, Atmos. Chem. Phys., 3, 713–723, https://doi.org/10.5194/acp-3-713-2003, 2003.

Diab, R. D., Thompson, A. M., Mari, K., Ramsay, L., and Coetzee, G. J. R.: Tropospheric ozone climatology over Irene, South Africa, from 1990 to 1994 and 1998 to 2002, J. Geophys. Res., 109, 20301–203012, https://doi.org/10.1029/2004JD004793, 2004.

Dufour, G., Hauglustaine, D., Zhang, Y., Eremenko, M., Cohen, Y., Gaudel, A., Siour, G., Lachatre, M., Bense, A., Bessagnet, B., Cuesta, J., Ziemke, J., Thouret, V., and Zheng, B.: Recent ozone trends in the Chinese free troposphere: role of the local emission reductions and meteorology, Atmos. Chem. Phys., 21, 16001–16025, https://doi.org/10.5194/acp-21-16001-2021, 2021.

European Centre for Medium-Range Weather Forecasts (ECMWF): ERA5: The Fifth Generation ECMWF Atmospheric Reanalysis of the Global Climate, Copernicus Climate Data Store (CDS) [data set], https://climate.copernicus.eu/climate-reanalysis, last access: 23 August 2023.

Ferm, M.: A Sensitive Diffusional Sampler, IVL Report L91, Swedish Environmental Research Institute, Göteborg, Sweden, 12 pp., ISSN 0283-877X, 1991.

Ferm, M. and Rodhe, H.: Measurements of Air Concentrations of $SO_2$, $NO_2$ and $NH_3$ at Rural and Remote Sites in Asia, J. Atmos. Chem., 27, 17–29, https://doi.org/10.1023/A:1005816621522, 1997.

Ferreira, J., Reeves, C. E., Murphy, J. G., Garcia-Carreras, L., Parker, D. J., and Oram, D. E.: Isoprene emissions modelling for West Africa: MEGAN model evaluation and sensitivity analysis, Atmos. Chem. Phys., 10, 8453–8467, https://doi.org/10.5194/acp-10-8453-2010, 2010.

Fleming, Z. L., Doherty, R. M., von Schneidemesser, E., Malley, C. S., Cooper, O. R., Pinto, J. P., Colette, A., Xu, X., Simpson, D., Schultz, M. G., Lefohn, A. S., Hamad, S., Moolla, R. Solberg, S., and Feng, Z.: Tropospheric Ozone Assessment Report: Present-day ozone distribution and trends relevant to human health, Elem. Sci. Anth., 6, 1–41 https://doi.org/10.1525/elementa.273, 2018.

Fowler, D., Pilegaard, K., Sutton, M. A., Ambus, P., Raivonen, M., Duyzer, J., Simpson, D., Fagerli, H., Fuzzi, S., Schjoerring, J. K., Granier, C., Neftel, A., Isaksen, I. S. A., Laj, P., Maione, M., Monks, P. S., Burkhardt, J., Daemmgen, U., Neirynck, J., Personne, E., Wichink-Kruit, R., Butterbach-Bahl, K., Flechard, C., Tuovinen, J. P., Coyle, M., Gerosa, G., Loubet, B., Altimir, N., Gruenhage, L., Ammann, C., Cieslik, S., Paoletti, E., Mikkelsen, T. N., Ro-Poulsen, H., Cellier, P., Cape, J. N., Horvath, L., Loreto, F., Niinemets, Ü., Palmer, P. I., Rinne, J., Misztal, P., Nemitz, E., Nilsson, D., Pryor, S., Gallagher, M. W., Vesala,

T., Skiba, U., Brüggemann, N., ZechmeisterBoltenstern, S., Williams, J., O'dowd, C., Facchini, M. C., De Leeuw, G., Flossman, A., Chaumerliac, N., and Erisman, J. W.: Atmospheric composition change: ecosystems-Atmosphere interactions, Atmos. Environ. 43, 5193–5267, foi:10.1016/j.atmosenv.2009.07.068, 2009.

Frimpong, B. F., Koranteng, A., and Molkenthin, F.: Analysis of temperature variability utilising Mann–Kendall and Sen's slope estimator tests in the Accra and Kumasi Metropolises in Ghana, Environmental Systems Research, 11, 1–13, https://doi.org/10.1186/s40068-022-00269-1, 2022.

Galanter, M., Levy I. I., H., and Carmichael, G. R.: Impacts of biomass burning on tropospheric CO, $NO_x$, and $O_3$, J. Geophys. Res., 105, 6633–6653, https://doi.org/10.1029/1999JD901113, 2000.

Galy-Lacaux, C. and Modi, A. I.: Precipitation Chemistry in the Sahelian Savanna of Niger, Africa, J. Atmos. Chem., 30, 319–343, 1998.

Galy-Lacaux, C., Laouali, D., Descroix, L., Gobron, N., and Liousse, C.: Long term precipitation chemistry and wet deposition in a remote dry savanna site in Africa (Niger), Atmos. Chem. Phys., 9, 1579–1595, https://doi.org/10.5194/acp-9-1579-2009, 2009.

Galy-Lacaux, C., Diop, B., Orange, D., Sanogo, S., Soumaguel, N., Kanouté, C.O., Gardrat, E., Dias Alves, M., Lenoir, O., Ossohou, M., Adon, M., and Al-Ourabi, H.: Trace gases, Katigoubou, Mali, Aeris [data set], https://doi.org/10.25326/604, 2023a.

Galy-Lacaux, C., Mougin, E., Maïga, H., Soumaguel, N., Delon, C., Gardrat, E., Dias Alves, M. Lenoir, O., and Lavenu, E.: Trace gases Agoufou, Mali, Aeris [data set], https://doi.org/10.25326/610, 2023b.

Galy-Lacaux, C., Dorego, G. S., Gardrat, E., Dias Alves, M., Lenoir, O., Der Ba, S., N'Diaye, G. R., Séné, M., Thiam, A., Féron, A., and Ossohou, M.: Trace gases, Bambey, Senegal, Aeris [data set], https://doi.org/10.25326/609, 2023c.

Galy-Lacaux, C., N'Diaye, O., Guiro, I., Ba, D., Delon, C., Gardrat, E., Dias Alves, M., Lenoir, O., and Ossohou, M.: Trace gases, Dahra, Senegal, Aeris [data set], https://doi.org/10.25326/606, 2023d.

Galy-Lacaux, C., Yoboué, V., Ossohou, M., Gardrat, E., Dias Alves, M., Lenoir, O., Konaté, I., Ki, A. F., Ouattara, A., Adon, M., Al-Ourabi, H., and Zouzou, R.: Trace gases, Lamto, Côte d'Ivoire, Aeris [data set], https://doi.org/10.25326/275, 2023e.

Galy-Lacaux, C., Tathy, J.-P., Opepa, C. K., Brncic, T., Gardrat, E., Dias Alves, M., and Lenoir, O.: Trace gases, Bomassa, Congo, Aeris [data set], https://doi.org/10.25326/607, 2023f.

Galy-Lacaux, C., Delon, C., Bakayoko, A., Gardrat, E., Dias Alves, M., and Okumu, S.: Trace gases, Mbita, Kenya, Aeris [data set], https://doi.org/10.25326/642, 2023g.

García-Lázaro, J., Moreno-Ruiz, J., Riaño, D., and Arbelo, M.: Estimation of burned area in the northeastern siberian boreal forest from a long-term data record (LTDR) 1982–2015 time series, Remote Sens. 10, 1–15, https://doi.org/10.3390/rs10060940, 2018.

Gaudel, A, Cooper, O. R., Ancellet, G., Barret, B., Boynard, A., Burrows, J. P., Clerbaux, C., Coheur, P.-F., Cuesta, Cuevas, J. E., Doniki, S., Dufour, Ebojie, G. F., Foret, Garcia, G. O., Granados-Muñoz, M. J., Hannigan, J. W., Hase, F., Hassler, B., Huang, G., Hurtmans, D., Jaffe, D., Jones, N., Kalabokas, P., Kerridge, B., Kulawik, S., Latter, B., Leblanc, T., Le Flochmoën, E., Lin, W., Liu, J., Liu, X., Mahieu, E., McClure-Begley, A., Neu, J. L., Osman, M., Palm, M., Petetin, H., Petropavlovskikh, I., Querel, R, Rahpoe, R. N., Rozanov, A., Schultz, M. G., Schwab, J., Siddans, R., Smale, D., Steinbacher, M., Tanimoto, H., Tarasick, D. W., Thouret, V., Thompson, A. M., Trick, T., Weatherhead, E., Wespes, C., Worden, H. M., Vigouroux, C., Xu, X., Zeng, G., and Ziemke, J.: Tropospheric Ozone Assessment Report: Present-day ozone distribution and trends relevant to climate and model evaluation, Elem. Sci. Anth., 6, 1–58, https://doi.org/10.1525/elementa.291, 2018.

Gaudel, A., Cooper, O. R., Chang, K.-L., Bourgeois, I., Ziemke, J. R., Strode, S. A., Oman, L. D., Sellitto, P., Nédélec, P., Blot, R., Thouret, V., and Granier, C.: Aircraft observations since the 1990s reveal increases of tropospheric ozone at multiple locations across the Northern Hemisphere, Sci. Adv., 6, 1–11, https://doi.org/10.1126/sciadv.aba8272, 2020.

Gaudel, A., Bourgeois, I., Li, M., Chang, K.-L., Ziemke, J., Sauvage, B., Stauffer, R. M., Thompson, A. M., Kollonige, D. E., Smith, N., Hubert, D., Keppens, A., Cuesta, J., Heue, K.-P., Veefkind, P., Aikin, K., Peischl, J., Thompson, C. R., Ryerson, T. B., Frost, G. J., McDonald, B. C., and Cooper, O. R.: Tropical tropospheric ozone distribution and trends from in situ and satellite data, Atmos. Chem. Phys., 24, 9975–10000, https://doi.org/10.5194/acp-24-9975-2024, 2024.

Graedel, T. E. and Crutzen, P. J.: Atmospheric Change: An Earth System Perspective, W. H. Freeman and Company, New York, NY, 446 pp., ISBN 0716723344, 1993.

Guenther, A., Karl, T., Harley, P., Wiedinmyer, C., Palmer, P. I., and Geron, C.: Estimates of global terrestrial isoprene emissions using MEGAN (Model of Emissions of Gases and Aerosols from Nature), Atmos. Chem. Phys., 6, 3181–3210, https://doi.org/10.5194/acp-6-3181-2006, 2006.

Hagenbjörk, A., Malmqvist, E., Mattisson, K., Sommar, N. J., and Modig, L.: The spatial variation of $O_3$, NO, $NO_2$ and $NO_x$ and the relation between them in two Swedish cities, Environ. Monit. Assess. 189, 161–172, https://doi.org/10.1007/s10661-017-5872-z, 2017.

Hamdun, A. M. and Arakaki T.: Analysis of Ground Level Ozone and Nitrogen Oxides in the City of Dar es Salaam and the Rural Area of Bagamoyo, Tanzania, Open Journal of Air Pollution, 4, 224–238, https://doi.org/10.4236/ojap.2015.44019, 2015.

Heue, K.-P., Coldewey-Egbers, M., Delcloo, A., Lerot, C., Loyola, D., Valks, P., and van Roozendael, M.: Trends of tropical tropospheric ozone from 20 years of European satellite measurements and perspectives for the Sentinel-5 Precursor, Atmos. Meas. Tech., 9, 5037–5051, https://doi.org/10.5194/amt-9-5037-2016, 2016.

Hirsch, R. M., Slack, J. R., and Smith, R. A.: Techniques of trend analysis for monthly water quality data, Water Resour. Res. 18, 107–121, https://doi.org/10.1029/WR018i001p00107, 1982.

Homyak P. M., Sickman, J. O., Miller, A. E., Melack, J. M., and Schimel, J. P.: Assessing N saturation in a seasonally dry chaparral watershed: Limitations of traditional indicators of N saturation, Ecosystems, 17, 1286–1305, https://doi.org/10.1007/s10021-014-9792-2, 2014.

Hou, X., Zhang, Y., Lv, X., and Lee, J.: The Impact of Meteorological Conditions and Emissions on Tropospheric Column Ozone Trends in Recent Years, Remote Sens., 15, 5293–5305, https://doi.org/10.3390/rs15225293, 2023.

Ihedike, C., Mooney, J. D., Fulton, J., and Ling, J.: Evaluation of real-time monitored ozone concentration from Abuja, Nigeria, BMC Public Health, 23, 1–7, https://doi.org/10.1186/s12889-023-15327-1, 2023.

Jaars, K., van Zyl, P. G., Beukes, J. P., Hellén, H., Vakkari, V., Josipovic, M., Venter, A. D., Räsänen, M., Knoetze, L., Cilliers, D. P., Siebert, S. J., Kulmala, M., Rinne, J., Guenther, A., Laakso, L., and Hakola, H.: Measurements of biogenic volatile organic compounds at a grazed savannah grassland agricultural landscape in South Africa, Atmos. Chem. Phys., 16, 15665–15688, https://doi.org/10.5194/acp-16-15665-2016, 2016.

Jaegle, L., Martin, R. V., Chance, K., Steinberger, L., Kurosu, T. P., Jacob, D. J., Modi, A. I., Yoboue, V., Sigha-Nkamdjou, L., and Galy-Lacaux, C.: Satellite mapping of rain-induced nitric oxide emissions from soils, J. Geophys. Res., 109, 1–10, https://doi.org/10.1029/2004JD004787, 2004.

Josipovic, M., Annegarn, H. J., Kneen, M. A., Pienaar, J. J., and Piketh, S. J.,: Concentrations, distributions and critical level exceedance assessment of $SO_2$, $NO_2$ and $O_3$ in South Africa, Environ. Monit. Assess., 171, 181–196, https://doi.org/10.1007/s10661-009-1270-5, 2010.

Kai, R. F., Scholes, M. C., Piketh, S. J., and Scholes, R. J.: Analysis of the first surface nitrogen dioxide concentration observations over the South African Highveld derived from the Pandora-2s instrument, Clean Air Journal, 32, 1–11, https://doi.org/10.17159/caj/2022/32/1.13242, 2022.

Keita, S., Liousse, C., Assamoi, E.-M., Doumbia, T., N'Datchoh, E. T., Gnamien, S., Elguindi, N., Granier, C., and Yoboué, V.: African anthropogenic emissions inventory for gases and particles from 1990 to 2015, Earth Syst. Sci. Data, 13, 3691–3705, https://doi.org/10.5194/essd-13-3691-2021, 2021.

Kendall, M. G.: Rank Correlation Methods, Charles Griffin, 4th edn., Charles Griffin, London, ISBN 9780852641996, 1975.

Khoder, M. I.: Diurnal, Seasonal and Weekdays-Weekends Variations of Ground Level Ozone Concentrations in an Urban Area in Greater Cairo, Environ. Monit. Assess., 149, 349–362, https://doi.org/10.1007/s10661-008-0208-7, 2009.

Kimayu, J. M., Gikuma-Njuru, P., and Musembi, D. K., : Temporal and Spatial Variability of Tropospheric Ozone in Nairobi City, Kenya, Physical Science International Journal, 13, 1–12, https://doi.org/10.9734/PSIJ/2017/31452, 2017.

Laakso, L., Laakso, H., Aalto, P. P., Keronen, P., Petäjä, T., Nieminen, T., Pohja, T., Siivola, E., Kulmala, M., Kgabi, N., Molefe, M., Mabaso, D., Phalatse, D., Pienaar, K., and Kerminen, V.-M.: Basic characteristics of atmospheric particles, trace gases and meteorology in a relatively clean Southern African Savannah environment, Atmos. Chem. Phys., 8, 4823–4839, https://doi.org/10.5194/acp-8-4823-2008, 2008.

Laakso, L., Vakkari, V., Virkkula, A., Laakso, H., Backman, J., Kulmala, M., Beukes, J. P., van Zyl, P. G., Tiitta, P., Josipovic, M., Pienaar, J. J., Chiloane, K., Gilardoni, S., Vignati, E., Wiedensohler, A., Tuch, T., Birmili, W., Piketh, S., Collett, K., Fourie, G. D., Komppula, M., Lihavainen, H., de Leeuw, G., and Kerminen, V.-M.: South African EUCAARI measurements: seasonal variation of trace gases and aerosol optical properties, Atmos. Chem. Phys., 12, 1847–1864, https://doi.org/10.5194/acp-12-1847-2012, 2012.

Laban, T. L., van Zyl, P. G., Beukes, J. P., Vakkari, V., Jaars, K., Borduas-Dedekind, N., Josipovic, M., Thompson, A. M., Kulmala, M., and Laakso, L.: Seasonal influences on surface ozone variability in continental South Africa and implications for air quality, Atmos. Chem. Phys., 18, 15491–15514, https://doi.org/10.5194/acp-18-15491-2018, 2018.

Laban, T. L., Van Zyl, P. G., Beukes, J. P., Mikkonen, S., Santana, L., Josipovic, M., Vakkari, Thompson, A. M., Kulmala, M., and Laakso L.: Statistical analysis of factors driving surface ozone variability over continental South Africa, J. Integr. Environ. Sci., 17, 1–28, https://doi.org/10.1080/1943815X.2020.1768550, 2020.

Lannuque, V., Sauvage, B., Barret, B., Clark, H., Athier, G., Boulanger, D., Cammas, J.-P., Cousin, J.-M., Fontaine, A., Le Flochmoën, E., Nédélec, P., Petetin, H., Pfaffenzeller, I., Rohs, S., Smit, H. G. J., Wolff, P., and Thouret, V.: Origins and characterization of CO and $O_3$ in the African upper troposphere, Atmos. Chem. Phys., 21, 14535–14555, https://doi.org/10.5194/acp-21-14535-2021, 2021.

Laouali, D., Galy-Lacaux, C., Gardrat, E., Dias Alves, M., Lenoir, O., Zakou, A., Ossohou, M., Adon, M., and Al-Ourabi, H.: Trace gases, Banizoumbou, Niger, Aeris [data set], https://doi.org/10.25326/608, 2023.

Laville, P., Henault, C., Gabrielle, B., and Serca, D.: Measurement and modelling of NO fluxes over maize and wheat crops during their growing seasons: effect of crop management, Nutr. Cycl. Agroecosyst. 72, 159–171, https://doi.org/10.1007/s10705-005-0510-5, 2005.

Lee, J. D., Squires, F. A., Sherwen, T., Wilde, S. E., Cliff, S. J., Carpenter, L. J., Hopkins, J. R., Bauguitte, S. J., Reed, C., Barker, P., Allen, G., Bannan, T. J., Matthews, E., Mehra, A., Percival, C., Heard, D. E., Whalley, L. K., Ronnie, G. V., Seldon, S., Ingham, T., Keller, C. A., Knowland, K. E., Nisbetj, E. G., and Andrewsab. S.: Ozone production and precursor emission from wildfires in Africa, Environ. Sci.: Atmos., 1, 524–542, https://doi.org/10.1039/D1EA00041A, 2021.

Lefohn, A. S., Malley, C. S., Smith, L., Wells, B., and Hazucha, M.: Tropospheric Ozone Assessment Report: Global ozone metrics for climate change, human health, and crop/ecosystem research, Elem. Sci. Anth., 6, 1–39 https://doi.org/10.1525/elementa.279, 2018.

Lelieveld, J., Evans, J. S., Fnais, M., Giannadaki, D., and Pozzer, A.: The contribution of outdoor air pollution sources to premature mortality on a global scale, Nature, 525, 367–371, https://doi.org/10.1038/nature15371, 2015.

Lin, M., Horowitz, L. W., Cooper, O. R., Tarasick, D., Conley, S., Iraci, L. T., Johnson, B., Leblanc, T., Petropavlovskikh, I., and Yates, E. L.: Revisiting the evidence of increasing springtime ozone mixing ratios in the free troposphere over western North America, Geophys. Res. Lett., 42, 8719–8728, https://doi.org/10.1002/2015GL065311, 2015.

Liu, Y., Schallhart, S., Taipale, D., Tykkä, T., Räsänen, M., Merbold, L., Hellén, H., and Pellikka, P.: Seasonal and diurnal variations in biogenic volatile organic compounds in highland and lowland ecosystems in southern Kenya, Atmos. Chem. Phys., 21, 14761–14787, https://doi.org/10.5194/acp-21-14761-2021, 2021.

Lourens, A. S., Beukes, J. P., Van Zyl, P. G., Fourie, G. D., Burger, J. W., Pienaar, J. J., Read, C. E., and Jordaan, J. H.: Spatial and temporal assessment of gaseous pollutants in the Highveld of South Africa, S. Afr. J. Sci., 107, 1–8, https://doi.org/10.4102/sajs.v107i1/2.269, 2011.

Lu, X., Zhang, L., Zhao, Y., Jacob, D. J., Hu, Y., Hu, L., Gao, M., Liu, X., Petropavlovskikh, I., McClure-Begley, A., and Querel, R.: Surface and tropospheric ozone trends in the Southern Hemisphere since 1990: possible linkages to poleward expansion of the Hadley circulation, Sci. Bull., 64, 400–409, https://doi.org/10.1016/j.scib.2018.12.021, 2019.

Ludwig, J., Meixner, F. X., Vogel, B., and Forstner, J.: Soil-air exchange of nitric oxide: An overview of processes, environmental factors, and modelling studies, Biogeochemistry, 52, 225–257, https://doi.org/10.1023/A:1006424330555, 2001.

Mari, C. H., Reeves, C. E., Law, K. S., Ancellet, G., Andres-Hernandez, M. D., Barret, B., Bechara, J., Borbon, A., Bouarar, I., Cairo, F., Commane, R., Delon, C., Evans, M. J., Fierli, F., Floquet, C., Galy-Lacaux, C., Heard, D. E., Homan, C. D., Ingham, T., Larsen, N., Lewis, A. C., Liousse, C., Murphy, J. G., Orlandi, E., Oram, D. E., Saunois, M., Serça, D., Stewart, D. J., Stone, D., Thouret, V., van Velthoven, P., and Williams, J. E.: Atmospheric composition of West Africa: highlights from the AMMA international program, Atmos. Sci. Let. 12, 13–18, https://doi.org/10.1002/asl.289, 2011.

Martins, J. J., Dhammapala, R. S., Lachmann, G., Galy-Lacaux, C., and Pienaar, J. J.: Long-term measurements of sulphur dioxide, nitrogen dioxide, ammonia, nitric acid and ozone in southern Africa using passive samplers, S. Afr. J. Sci., 103, 336–342, https://hdl.handle.net/10520/EJC96693 (last access: 16 June 2024), 2007.

Mayaux, P., Bartholomeì, E., Fritz, S., and Belward, A.: A new land-cover map of Africa for the year 2000: New land-cover map of Africa, J. Biogeogr., 31, 861–877, https://doi.org/10.1111/j.1365-2699.2004.01073.x, 2004.

Merabtene, T., Siddique, M., and Shanableh, A.: Assessment of seasonal and annual rainfall trends and variability in sharjah city, UAE. Adv. Meteorol., 2016, 1–13, https://doi.org/10.1155/2016/6206238, 2016.

Mills, G., Pleijel, H., Malley, C. S., Sinha, B., Cooper, O. R., Schultz, M. G., Neufeld, H. S., Simpson, D., Sharps, K., Feng, Z., Gerosa, G., Harmens, H., Kobayashi, K., Saxena, P., Paoletti, E., Sinha, V., and Xu, X.: Tropospheric Ozone Assessment Report: Present-day tropospheric ozone distribution and trends relevant to vegetation, Elem. Sci. Anth., 6, 1–46, https://doi.org/10.1525/elementa.302, 2018.

Monks, P. and Leigh, R.: Tropospheric chemistry and air pollution, in: Atmospheric Science for Environmental Scientists, edited by: Hewitt, C. N. and Jackson, A. V., Wiley-Blackwell, Oxford, UK, 300 pp., ISBN 978140518542-4, 2009.

Monks, P. S., Archibald, A. T., Colette, A., Cooper, O., Coyle, M., Derwent, R., Fowler, D., Granier, C., Law, K. S., Mills, G. E., Stevenson, D. S., Tarasova, O., Thouret, V., von Schneidemesser, E., Sommariva, R., Wild, O., and Williams, M. L.: Tropospheric ozone and its precursors from the urban to the global scale from air quality to short-lived climate forcer, Atmos. Chem. Phys., 15, 8889–8973, https://doi.org/10.5194/acp-15-8889-2015, 2015.

Morakinyo, O. M., Mukhola, M. S., and Mokgobu, M. I.: Ambient Gaseous Pollutants in an Urban Area in South Africa: Levels and Potential Human Health Risk, Atmosphere, 11, 1–14, https://doi.org/10.3390/atmos11070751, 2020.

Mulumba, J.-P., Venkataraman, S., and Thomas, J. O.: Modeling Tropospheric Ozone Climatology over Irene (South Africa) Using Retrieved Remote Sensing and Ground-Based Measurement Data, J. Remote Sens. GIS, 4, 151, https://doi.org/10.4172/2469-4134.1000151, 2015.

Ngoasheng, M., Beukes, J. P., van Zyl, P. G., Swartz, J.-S., Loate, V., Krisjan, P., Mpambani, S., Kulmala, M., Vakkari, V., and Laakso, L.: Assessing $SO_2$, $NO_2$ and $O_3$ in rural areas of the North West Provinc. Clean Air Journal, 31, 1–14, https://doi.org/10.17159/caj/2021/31/1.9087, 2021.

Ojumu, A. M.: Transport of Nitrogen Oxides and Nitric Acid Pollutants over South Africa and Air Pollution in Cape Town, MSc, University of South Africa, 68 pp., https://uir.unisa.ac.za/handle/10500/11911 (last access: 13 April 2023), 2013.

Oltmans, S. J., Lefohn, A. S., Shadwick, D., Harris, J. M., Scheel, H. E., Galbally, I., Tarasick, D. W., Johnson, B. J., Brunke, E. G., Claude, H., Zeng, G., Nichol, S., Schmidlin, F., Davies, J., Cuevas, E., Redondas, A., Naoe, H., Nakano, T., and Kawasato, T.: Recent tropospheric ozone changes-A pattern dominated by slow or no growth, Atmos. Environ., 67, 331–351, https://doi.org/10.1016/j.atmosenv.2012.10.057, 2013.

Oluleye, A. and Okogbue, E. C.: Analysis of temporal and spatial variability of total column ozone over West Africa using daily TOMS measurements, Atmos. Pollut. Res., 4, 387–397, https://doi.org/10.5094/APR.2013.044, 2013.

Ossohou M., C. Galy-Lacaux, C., V. Yoboué, V., Hickmanc, J. E., Gardrat, E., Adona, M., Darrasi, S., Laoualie, D., Akpod, A., Ouafo, M., Diopg, B., and Opepah, C.: Trends and seasonal variability of atmospheric NO and HNO concentrations across three major African biomes inferred from long-term series of ground-based and satellite measurements, Atmos. Environ., 207, 148–66, https://doi.org/10.1016/j.atmosenv.2019.03.027, 2019.

Ouafo-Leumbe, M.-R., Galy-Lacaux, C., Sigha-Nkamdjou, L., Gardrat, E., Dias Alves, M., Lenoir, O., Meka, M. Z., and Amougou, M.: Trace gases, Zoétélé, Cameroon, Aeris [data set], https://doi.org/10.25326/603, 2023.

Petäjä, T., Vakkari, V., Pohja, T., Nieminen, T., Laakso, H., Aalto, P. P., Keronen, P., Siivola, E., Kerminen, V.-M., Kulmala, M., and Laakso, L.: Transportable Aerosol Characterization Trailer with Trace Gas Chemistry: Design, Instruments and Verification, Aerosol Air Qual. Res., 13, 421–435, https://doi.org/10.4209/aaqr.2012.08.0207, 2013.

Petetin, H., Bowdalo, D., Bretonnière, P.-A., Guevara, M., Jorba, O., Mateu Armengol, J., Samso Cabre, M., Serradell, K., Soret, A., and Pérez Garcia-Pando, C.: Model output statistics (MOS) applied to Copernicus Atmospheric Monitoring Service (CAMS) $O_3$ forecasts: trade-offs between continuous and categorical skill scores, Atmos. Chem. Phys., 22, 11603–11630, https://doi.org/10.5194/acp-22-11603-2022, 2022.

Rummel, U., Ammann, C., Kirkman, G. A., Moura, M. A. L., Foken, T., Andreae, M. O., and Meixner, F. X.: Seasonal variation of ozone deposition to a tropical rain forest in southwest Amazonia, Atmos. Chem. Phys., 7, 5415–5435, https://doi.org/10.5194/acp-7-5415-2007, 2007.

Sadiq, M., Tai, A. P. K., Lombardozzi, D., and Val Martin, M.: Effects of ozone–vegetation coupling on surface ozone air quality via biogeochemical and meteorological feedbacks, Atmos. Chem. Phys., 17, 3055–3066, https://doi.org/10.5194/acp-17-3055-2017, 2017.

Salem, A. A., Soliman, A. A., and El-Haty, I. A.: Determination of nitrogen dioxide, sulfur dioxide, ozone, and ammonia in ambient air using the passive sampling method associated with ion

chromatographic and potentiometric analyses, Air Qual. Atmos. Health, 2, 133–145, https://doi.org/10.1007/s11869-009-0040-4, 2009.

Saunois, M., Reeves, C. E., Mari, C. H., Murphy, J. G., Stewart, D. J., Mills, G. P., Oram, D. E., and Purvis, R. M.: Factors controlling the distribution of ozone in the West African lower troposphere during the AMMA (African Monsoon Multidisciplinary Analysis) wet season campaign, Atmos. Chem. Phys., 9, 6135–6155, https://doi.org/10.5194/acp-9-6135-2009, 2009.

Sauvage, B., Thouret, V., Cammas, J.-P., Gheusi, F., Athier, G., and Nédélec, P.: Tropospheric ozone over Equatorial Africa: regional aspects from the MOZAIC data, Atmos. Chem. Phys., 5, 311–335, https://doi.org/10.5194/acp-5-311-2005, 2005.

Sauvage, B., Gheusi, F., Thouret, V., Cammas, J.-P., Duron, J., Escobar, J., Mari, C., Mascart, P., and Pont, V.: Medium-range mid-tropospheric transport of ozone and precursors over Africa: two numerical case studies in dry and wet seasons, Atmos. Chem. Phys., 7, 5357–5370, https://doi.org/10.5194/acp-7-5357-2007, 2007.

Saxton, J. E., Lewis, A. C., Kettlewell, J. H., Ozel, M. Z., Gogus, F., Boni, Y., Korogone, S. O. U., and Serça, D.: Isoprene and monoterpene measurements in a secondary forest in northern Benin, Atmos. Chem. Phys., 7, 4095–4106, https://doi.org/10.5194/acp-7-4095-2007, 2007.

Schultz, M. G., Schröder, S., Lyapina, O., Cooper, O. R., Galbally, I., Petropavlovskikh, I., von Schneidemesser, E., Tanimoto, H., Elshorbany, Y., Naja, M., Seguel, R. J., Dauert, U., Eckhardt, P., Feigenspan, S., Fiebig, M., Hjellbrekke, A.-G., Hong, Y.-D., Kjeld, P. C., Koide, H., Lear, G., Tarasick, D., Ueno, M., Wallasch, M., Baumgardner, D., Chuang, M.-T., Gillett, R., Lee, M., Molloy, S., Moolla, R., Wang, T., Sharps, K., Adame, J. A., Ancellet, G., Apadula, F., Artaxo, P., Barlasina, M. E., Bogucka, M., Bonasoni, P., Chang, L., Colomb, A., Cuevas-Agulló, E., Cupeiro, M., Degorska, A., Ding, A., Fröhlich, M., Frolova, M., Gadhavi, H., Gheusi, F., Gilge, S., Gonzalez, M. Y., Gros, V., Hamad, S. H., Helmig, D., Henriques, D., Hermansen, O., Holla, R., Hueber, J., Im, U., Jaffe, D. A., Komala, N., Kubistin, D., Lam, K.-S., Laurila, T., Lee, H., Levy, I., Mazzoleni, C., Mazzoleni, L. R., McClure-Begley, A., Mohamad, M., Murovec, M., Navarro-Comas, M., Nicodim, F., Parrish, D., Read, K. A., Reid, N., Ries, L., Saxena, P., Schwab, J. J., Scorgie, Y., Senik, I., Simmonds, P., Sinha, V., Skorokhod, A. I., Spain, G., Spang, W., Spoor, R., Springston, S. R., Steer, K., Steinbacher, M., Suharguniyawan, E., Torre, P., Trickl,T., Weili, L., Weller, R., Xiaobin, X., Xue, L., and Zhiqiang, M.: Tropospheric Ozone Assessment Report: Database and metrics data of global surface ozone observations, Elem. Sci. Anth., 5, 1–26, https://doi.org/10.1525/elementa.244, 2017.

Sen, P. K.: Estimates of the regression coefficient based on Kendall's tau, J. Am. Stat. Assoc. 63, 1379–1389, https://doi.org/10.2307/2285891, 1968.

Serca, D., Guenther, A., Klinger, L., Vierling, L., Harley, P., Druilhet, A., Greenberg, J., Baker, B., Baugh, W., Bouka-Biona, C., and Loemba-Ndembi, J.: EXPRESSO flux measurements at upland and lowland Congo tropical forest site, Tellus B, 53, 220–234, https://doi.org/10.3402/tellusb.v53i3.16593, 2001.

Silva, S. J. and Heald, C. L.: Investigating Dry Deposition of $O_3$ to Vegetation, J. Geophys. Res.-Atmos., 123, 559–573, https://doi.org/10.1002/2017JD027278, 2018.

Sindelarova, K., Granier, C., Bouarar, I., Guenther, A., Tilmes, S., Stavrakou, T., Müller, J.-F., Kuhn, U., Stefani, P., and Knorr, W.: Global data set of biogenic VOC emissions calculated by the MEGAN model over the last 30 years, Atmos. Chem. Phys., 14, 9317–9341, https://doi.org/10.5194/acp-14-9317-2014, 2014.

Singh, H. B., Herlth, D., Kolyer, R., Chatfield, R., Viezee, W., Salas, L. J., Chen, Y., Bradshaw, J. D., Sandholm, S. T., Talbot, R., Gregory, G. L., Anderson, B., Sachse, G. W., Browell, E., Bachmeier, A. S., Blake, D. R., Heikes, B., Jacob, D., and Fuelberg, H. E.: Impact of biomass burning emissions on the composition of the South Atlantic troposphere: Reactive nitrogen and ozone, J. Geophys. Res.-Atmos., 101, 24203–24219, https://doi.org/10.1029/96JD01018, 1996.

Sivakumar, V. and Ogunniyi, J.: Ozone climatology and variability over Irene, South Africa determined by ground based and satellite observations. Part 1: Vertical variations in the troposphere and stratosphere, Atmósfera, 30, 337–353, https://doi.org/10.20937/atm.2017.30.04.05, 2017.

Sofen, E. D., Bowdalo, D., and Evans, M. J.: How to most effectively expand the global surface ozone observing network, Atmos. Chem. Phys., 16, 1445–1457, https://doi.org/10.5194/acp-16-1445-2016, 2016.

Stauffer, R. M., Thompson, A. M., Kollonige, D. E., Komala, N., Al-Ghazali, H. K., Risdianto, D. Y., Dindang, A., Fairudz bin Jamaluddin, A., Sammathuria, M. K., Zakaria, N. B., Johnson, B. J., and Cullis, P. D.: Dynamical drivers of free-tropospheric ozone increases over equatorial Southeast Asia, Atmos. Chem. Phys., 24, 5221–5234, https://doi.org/10.5194/acp-24-5221-2024, 2024.

Stewart, D. J., Taylor, C. M., Reeves, C. E., and McQuaid, J. B.: Biogenic nitrogen oxide emissions from soils: impact on $NO_x$ and ozone over west Africa during AMMA (African Monsoon Multidisciplinary Analysis): observational study, Atmos. Chem. Phys., 8, 2285–2297, https://doi.org/10.5194/acp-8-2285-2008, 2008.

Swap, R. J., Annegarn, H. J., Suttles, J. T., King, M. D., Platnick, S., Privette, J. L., and Scholes, R. J.: Africa burning: a thematic analysis of the southern African regional science initiative (SAFARI 2000), J. Geophys. Res., 108, 1–15, https://doi.org/10.1029/2003JD003747, 2003.

Swartz, J.-S., van Zyl, P. G., Beukes, J. P., Galy-Lacaux, C., Ramandh, A., and Pienaar, J. J.: Measurement report: Statistical modelling of long-term trends of atmospheric inorganic gaseous species within proximity of the pollution hotspot in South Africa, Atmos. Chem. Phys., 20, 10637–10665, https://doi.org/10.5194/acp-20-10637-2020, 2020a.

Swartz, J.-S., Van Zyl, P. G., Beukes, J. P., Labuschagne, C., Brunke, E.-G., Galy-Lacaux, C., Pienaar, J. J., and Portafaix, T.: Twenty-one years of passive sampling monitoring of $SO_2$, $NO_2$ and $O_3$ at the Cape Point GAW station, South Africa, Atmos. Environ. 222, 1–17, https://doi.org/10.1016/j.atmosenv.2019.117128, 2020b.

Tarasick, D., Galball, I. E., Cooper, O. R., Schultz, M. G., Ancellet, G., Leblanc, T., Wallington, T. J., Ziemke, J., Liu, X., Steinbacher, M., Staehelin, J., Vigouroux, C., Hannigan, J. W., García, O., Foret, G., Zanis, P., Weatherhead, E., Petropavlovskikh, I., Worden, H., Osman, M., Liu, J., Chang, K.-L., Gaudel, A., Lin, M., Granados-Muñoz, M., Thompson, A. M., Oltmans, S. J., Cuesta, J., Dufour, G., Thouret, V., Hassler, B., Trick T., and Neu, J. L.: Tropospheric Ozone Assess-

ment Report: Tropospheric ozone from 1877 to 2016, observed levels, trends and uncertainties, Elem. Sci. Anth., 7, 1–72, https://doi.org/10.1525/elementa.376, 2019.

Thompson, A. M., Witte, J. C., Oltmans, S. J., Schmidlin, F. J., Logan, J. A., Fujiwara, M., Kirchhoff, V. W. J. H., Posny, F., Coetzee, G. J. R., Hoegger, B., Kawakami, S., Ogawa, T., Fortuin, J. P. F., and Kelder H. M.: Southern Hemisphere Additional Ozonesondes (SHADOZ) 1998–2000 tropical ozone climatology. 2. Tropospheric variability and the zonal wave-one, J. Geophys. Res., 108, 1-21, https://doi.org/10.1029/2002JD002241, 2003.

Thompson, A. M., Balashov, N. V., Witte, J. C., Coetzee, J. G. R., Thouret, V., and Posny, F.: Tropospheric ozone increases over the southern Africa region: bellwether for rapid growth in Southern Hemisphere pollution?, Atmos. Chem. Phys., 14, 9855–9869, https://doi.org/10.5194/acp-14-9855-2014, 2014.

Thompson, A. M., Stauffer, R. M., Wargan, K., Witte, J. C., Kollonige, D. E., and Ziemke, J. R.: Regional and seasonal trends in tropical ozone from SHADOZ profiles: Reference for models and satellite products, J. Geophys. Res., 126, 1–19, https://doi.org/10.1029/2021JD034691, 2021.

Tiitta, P., Vakkari, V., Croteau, P., Beukes, J. P., van Zyl, P. G., Josipovic, M., Venter, A. D., Jaars, K., Pienaar, J. J., Ng, N. L., Canagaratna, M. R., Jayne, J. T., Kerminen, V.-M., Kokkola, H., Kulmala, M., Laaksonen, A., Worsnop, D. R., and Laakso, L.: Chemical composition, main sources and temporal variability of $PM_1$ aerosols in southern African grassland, Atmos. Chem. Phys., 14, 1909–1927, https://doi.org/10.5194/acp-14-1909-2014, 2014.

Tsivlidou, M., Sauvage, B., Bennouna, Y., Blot, R., Boulanger, D., Clark, H., Le Flochmoën, E., Nédélec, P., Thouret, V., Wolff, P., and Barret, B.: Tropical tropospheric ozone and carbon monoxide distributions: characteristics, origins, and control factors, as seen by IAGOS and IASI, Atmos. Chem. Phys., 23, 14039–14063, https://doi.org/10.5194/acp-23-14039-2023, 2023.

Vakkari, V., Beukes, J. P., Laakso, H., Mabaso, D., Pienaar, J. J., Kulmala, M., and Laakso, L.: Long-term observations of aerosol size distributions in semi-clean and polluted savannah in South Africa, Atmos. Chem. Phys., 13, 1751–1770, https://doi.org/10.5194/acp-13-1751-2013, 2013.

van Zyl, P. G., Jaars, K., Beukes, J. P., Pienaar, J. J., Fourie, G. D., van der Walt, H. J., Mkhatshwa, G. V., van der Merwe, C., and James, C.: Trace gases, Louis Trichardt, South Africa, Aeris [data set], https://doi.org/10.25326/646, 2024a.

van Zyl, P. G., Jaars, K., Beukes, J. P., Pienaar, J. J., Fourie, G. D., van der Walt, H. J., Mkhatshwa, G. V., van der Merwe, C., Govender, N., Kubheka, W., Gardiner, E., and Tleane, J.: Trace gases, Skukuza, South Africa, Aeris [data set], https://doi.org/10.25326/645, 2024b.

van Zyl, P. G., Jaars, K., Beukes, J. P., Pienaar, J. J., Labuschagne, C., Mkololo, T., Brunke, E.-G., and Joubert, W.: Trace gases, Cape Point, South Africa, Aeris [data set], https://doi.org/10.25326/644, 2024c.

van Zyl, P. G., Jaars, K., Beukes, J. P., Pienaar, J. J., Fourie, G. D., van der Walt, H. J., Mkhatshwa, G. V., van der Merwe, C., and Deacon, M.: Trace gases, Amersfoort, South Africa, Aeris [data set], https://doi.org/10.25326/647, 2024d.

Vet, R., Artx, R. S., Carou, S., Shaw, M., Ro, C., Aas, W., Baker, A., Bowersox, V. C., Dentener, F., Galy-Lacaux, C., Hou, A., Pienaar, J.J., Gillet, R., Forti, M. C., Gromov, S., Hara, H., Khodzher, T., Mahowald, N. M., Nickovic, S., Rao, P. S. P., and Reid, N. W.: A global assessment of precipitation chemistry and deposition of sulfur, nitrogen, sea salt, base cations, organic acids, acidity and pH, and phosphorus, Atmos. Environ, 93, 3–100, https://doi.org/10.1016/j.atmosenv.2013.10.060, 2014.

Vitolo, C., Di Giuseppe, F., and D'Andrea, M.: Caliver: an R package for CALIbration and VERification of forest fire gridded model outputs, PLoS ONE, 13, 1–18, https://doi.org/10.1371/journal.pone.0189419, 2018.

Williams, J. E., Scheele, M. P., van Velthoven, P. F. J., Cammas, J.-P., Thouret, V., Galy-Lacaux, C., and Volz-Thomas, A.: The influence of biogenic emissions from Africa on tropical tropospheric ozone during 2006: a global modeling study, Atmos. Chem. Phys., 9, 5729–5749, https://doi.org/10.5194/acp-9-5729-2009, 2009.

Young, P. J., Archibald, A. T., Bowman, K. W., Lamarque, J.-F., Naik, V., Stevenson, D. S., Tilmes, S., Voulgarakis, A., Wild, O., Bergmann, D., Cameron-Smith, P., Cionni, I., Collins, W. J., Dalsøren, S. B., Doherty, R. M., Eyring, V., Faluvegi, G., Horowitz, L. W., Josse, B., Lee, Y. H., MacKenzie, I. A., Nagashima, T., Plummer, D. A., Righi, M., Rumbold, S. T., Skeie, R. B., Shindell, D. T., Strode, S. A., Sudo, K., Szopa, S., and Zeng, G.: Corrigendum to "Pre-industrial to end 21st century projections of tropospheric ozone from the Atmospheric Chemistry and Climate Model Intercomparison Project (ACCMIP)" published in Atmos. Chem. Phys., 13, 2063–2090, 2013, Atmos. Chem. Phys., 13, 5401–5402, https://doi.org/10.5194/acp-13-5401-2013, 2013.

Young, P. J., Naik, V., Fiore, A. M., Gaudel, A., Guo, J., Lin, M. Y., Neu, J. L., Parrish, D. D., Rieder, H. E., Schnell, J. L., Tilmes, S., Wild, O., Zhang, L., Ziemke, J., Brandt, J., Delcloo, A., Doherty, R. M., Geels, C., Hegglin, M. I., Hu, L., Im, U., Kumar, R., Luhar, A., Murray, L., Plummer, D., Rodriguez, J., Saiz-Lopez, A., Schultz, M. G., Woodhouse M. T., and Zeng G.: Tropospheric Ozone Assessment Report: Assessment of global-scale model performance for global and regional ozone distributions, variability, and trends, Elem. Sci. Anth., 6, 1–49, https://doi.org/10.1525/elementa.265, 2018.

Zhang, Y., Cooper, O. R., Gaudel, A., Thompson, A. M., Nédélec, P., Ogino, S.-Y., and West, J. J.: Tropospheric ozone change from 1980 to 2010 dominated by equatorward redistribution of emissions, Nat. Geosci., 9, 875–879, https://doi.org/10.1038/ngeo2827, 2016.

Zilbermann, N., Granier, C., Darras, S., and Liousse, C.: The ECCAD Database: Emissions of Atmospheric Compounds and Compilation of Ancillary Data, AERIS, https://eccad.sedoo.fr/#/data, last access: 24 October 2024.

Zunckel, M., Venjonoka, K., Pienaar, J. J., Brunke, E. G., Pretorius, O., Koosialee, A., Raghunandan, A., and van Tienhoven, A. M.: Surface ozone over southern Africa: synthesis of monitoring results during the cross-border air pollution impact assessment project, Atmos, Environ., 38, 6139–6147, https://doi.org/10.1016/j.atmosenv.2004.07.029, 2004.